Hydro-sedimentary dysfunctions as a key factor for the storage of contaminants in mountain rivers (Bienne River, Jura Mountains, France)

Elie Dhivert, André-Marie Dendievel, Marc Desmet, Bertrand Devillers, Cécile Grosbois

Version of Record: https://www.sciencedirect.com/science/article/pii/S0341816222001084
Manuscript_1147c8bddec230c5d3b1e7f95c4b70d3

Hydro-sedimentary dysfunctions as a key factor for the storage of contaminants in mountain rivers (Bienne River, Jura Mountains, France)

Elie DHIVERT[(1)(2)], André-Marie DENDIEVEL[(3)], Marc DESMET[(1)], Bertrand DEVILLERS[(4)], Cécile GROSBOIS[(1)]

(1) Université de Tours, EA 6293 GéoHydrosystèmes continentaux, F-37200 Tours, France
(2) Anthroposed, Groupe Coopetic, 39130 Etival, France
(3) Univ Lyon, Université Claude Bernard Lyon 1, CNRS, ENTPE, UMR 5023 LEHNA, F-69518 Vaulx-en-Velin, France.
(4) Parc naturel régional du Haut-Jura, 429 Le Village, 39310 Lajoux, France

Corresponding authors: elie.dhivert@gmail.com

Highlights:

- Sedimentological, metallic and organic contaminants analyses in riverbank sediments
- FingerPro unmixed model to assess geochemical fingerprinting
- Storage of legacy sediments along the banks since the 1950s
- Low transport capacity of contaminant bounded particles
- Strong decrease of the contamination gradient 60 km downstream of hotspot

Graphical abstract:

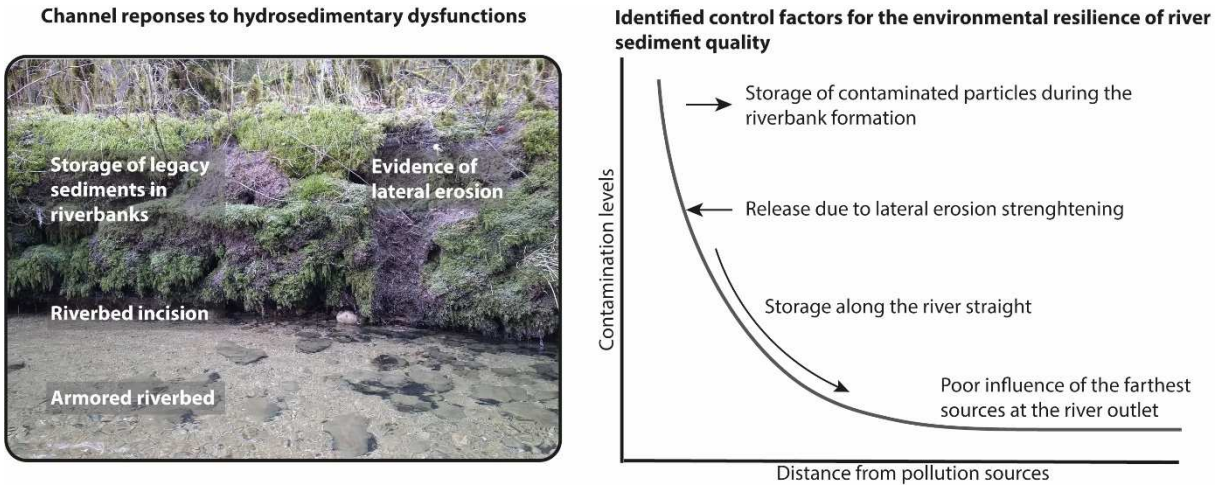

Abstract:

As within many European rivers in mountainous areas, the Bienne River (Jura Mountains, France) has been severely impacted by the implementation of obstacles to river flow. The aim of this study is to better understand how hydro-sedimentary dysfunctions (complex alterations of sediment transport in response to river engineering) can influence contaminants storage along the river. The sediment pollution trajectory was reconstructed based (1) on a well-dated sediment core, and (2) on several sediment samples taken at different depths on six riverbank profiles. Age control was established with a well-defined ^{137}Cs profile and time-related grain size transitions in the sediment core, and only

relatively for riverbank profiles using a plasticizer and PCB contents as chemical markers of the Anthropocene. Riverbanks and the core are composed of fine-grained legacy sediments deposited during the 20th century. They covered the former active channel mostly composed of pebbles and cobbles. Historical contaminants were the highest in the most upstream station and declined in the downstream direction to reach relatively low values in the lower river section. This historical upstream signal poorly influences the geochemical composition of sediments in the lower reaches, due its attenuation by numerous human-made obstacles to river flow and to the limited sediment transport capacity of the river. According to an unmixing model, the contribution of the upper sediments only weights a small percentage of the sedimentary mixture at the river outlet. These results highlight the sedimentary storage capacity of historical contaminants in mountain coarse-bedded river. This phenomenon has been led by a riverbed narrowing and stabilization caused by deep alterations of hydro-sedimentary processes. It finally emphasizes storage of sedimentary contaminants and leads to limited source influences. Hence, this study shows the key role of sedimentary transport, which triggers spatial and temporal variability of contaminants stored in sediments.

Key words:
Trace metal elements, polychlorinated biphenyls, di(2-ethylhexyl) phthalate, Sediment transport, Riverbank storage; Legacy sediments, Hydro-sedimentary alteration

1. Introduction

Since the 19th century, river systems have been impacted by an increase of human-induced pressure, and their natural functioning has been widely modified (Best, 2019). The cumulative impacts of anthropogenic activities intensified after 1945 and marked a great acceleration associated to the Anthropocene Epoch in Europe (Meybeck, 2003; Steffen et al., 2004; 2007; 2015; Downs and Piégay, 2019).

Hence, river engineering has greatly intensified during this period. River infrastructure such as weirs, sluices, dams, sills, embankments, and road culverts have become ubiquitous, especially in Europe (Tockner et al., 2009; Grill et al., 2019; Belletti et al., 2020). They have often led to significant deceleration of sediment transport at a catchment scale, expressed as a dramatic decrease in sedimentary discharges (Vörösmarty et al., 2003; Walling, 2009; Sokolov et al., 2020; Bussi et al., 2021), and marked by an increase in fine-grained (<63 µm) sediment deposition in floodplains and upstream of dams (Arnaud Fassetta, 2003; Provansal et al., 2014; Arnaud et al., 2019; Vauclin et al., 2019).

In response, significant changes of river courses occurred (Piégay, 2016; Versaci et al., 2018; Horacio et al., 2019; Piégay et al., 2020; Fazelpoor et al., 2021). Channel incision and narrowing have been documented for several decades. River engineering activities may have contributed to the interruption of the long-term geomorphic trajectory of channels adjustments and floodplains widening (Gasowski, 1994; Petit et al., 1996; Surian and Rinaldi, 2003; Latapie et al., 2014; Habersack et al., 2016; James, 2017).

Such alterations of the river sediment transport capacity (human-induced) and the associated geomorphological responses can be summarized as hydro-sedimentary dysfunctions in relation to river fragmentation and flow regulation (Grill et al., 2015; Jumani et al., 2020).

In river systems, the Anthropocene is also characterized by an important alteration of water and sediment chemical compositions, related to a large-scale increase of pollutant release in terms of source intensity, contaminant diversity, and impacted areas (Meybeck, 2002; Gałuszka et al., 2014;

Meybeck et al., 2018; Kaushal et al., 2018). Some of the pollutants emitted over time are bounded and sorbed to particles and can be stored in sediments for decades, centuries or even millennia. According to these properties, pollutant history can be revealed by studying sedimentary deposits (Charles and Hites, 1987; Heim and Schwarzbauer, 2013). These deposits can provide information about spatial and temporal changes in sedimentary contaminants at catchment scales (e.g. for French basins: Le Cloarec et al., 2011; Grosbois et al., 2012; Desmet et al., 2012; Mourier et al., 2014; Dhivert et al., 2016; Lorgeoux et al., 2016; Mourier et al., 2019; Dendievel et al., 2020ab; Gardes et al., 2020; Thiebault et al., 2021; Vauclin et al., 2021). They may also provide information about long-term changes in depositional environments (Bábek et al., 2008, 2020; Dhivert et al., 2015ab; Vauclin et al., 2020a).

Along mountain rivers, many studies have examined coarse sediment supply and transport, as well as the morpho-dynamic incidences of strong alterations (Lenzi et al., 2006; Recking, 2012; Yager et al., 2012; Attal, 2017). In these river systems, a high bedload concentration is important to maintain the steady-state conditions and to preserve the sedimentary balance at the catchment scale. By exceeding a certain threshold in the sediment transport decline, incised single-thread and armored channels can typically replace braided streams (Pitlick et al., 2008; Mueller and Pitlick, 2013). Changes in the bankfull shear stress can be observed and may influence the storage capacity of fine-grained sediments. Many pollutants, such as metallic contaminants, are primarily transported with fine-grained particles in the wash load. The settling capacity of this fine fraction controls the distribution of sedimentary pollutants (Horowitz and Elrick, 1997; Walling et al., 2003).

In this study, we focused on the longitudinal distribution of trace element (TEs) contaminations and some organic contaminants specific the Anthropocene as the di(2-ethylhexyl) phthalate (DEHP) and indicator polychlorinated biphenyls (PCBs) deposited in riverbanks along the Bienne River. This river basin serves as an interesting case study to understand the sedimentary transport of contaminants along the course of a coarse bedded river by studying cascading sediment transport. In brief, the Bienne River is a typical mountain river with a wide range of discharge and fluvial styles from straight channel in steep slope sections to more meandering channel where the floodplain is larger. Many dams, sills and embankments have been built in the river and their tributaries, with also infrastructures on slopes. In addition, several polluting industries are implanted in the Bienne catchment for decades. In this specific context, the principal objectives of this study are to analyze:

(i) long-term storage of sediments along riverbanks and associated contaminants,
(ii) spatial influence of contaminant sources, and
(iii) up-to-downstream trajectories at a basin scale to understand the sedimentary cascade of pollutants under the influence of infrastructures.

The novelty of this paper is to question the influence of human-induced alteration of sediment transport on the storage of contaminants in sediments at a river straight scale. This issue will go beyond the classical approach, traditionally focusing on a most downstream sampling site to reconstruct pollution trajectories at a basin scale. It is particularly justified for mountain rivers with a high density of infrastructure controlling large sections of river courses, as in many basins in Europe.

2. Study area

The Bienne River is 69 km long and drains a hydrogeological basin of 808 km² in the southern Jura Mountains of France (Fig. 1a). This is a mid-altitude mountain basin (elevations ranging between 304 and 1495 m a.s.l.) characterized by sedimentary rocks (Mesozoic limestones and marls, and glacial deposits dating back to the last glacial maximum in Western Europe). Groundwater flows are

particularly important because of a well-developed karstic system. The course of the river can be divided into two parts. The upper basin lies between the source spring and the town of Saint-Claude (draining an area of 392 km²). In this section, the Bienne River is confined within gorges (about 2000 m wide and 400 m deep) and the mean river slope is 12.4‰. A steep stream morphology can be recognized (Church and Zimmermann, 2007), with a straight channel and step pool patterns accentuated by numerous barriers to the river flow. The bedload is mostly composed of boulders and cobbles. The lower basin extends from Saint-Claude to Chancia (a village located at the Bienne River outlet in the Coiselet reservoir), where the valley is broader with a mean slope of 3.3‰ (draining an area of 416 km², Fig. 1b). In this section, the Bienne River channel is more meandering with scroll bars and sporadic islands. Large parts of this section are under the influence of dams. The bedload is essentially composed of pebbles and cobbles. The floodplain is only well-developed in less confined parts of the valley. It is discontinuous, mostly controlled by the bedrock and human settlements. Overflows are constrained in a narrow band of few dozen to hundred meters wide because of numerous embankments. Downstream of Chancia, the Bienne River finally meets the Ain River at the Coiselet reservoir (Rhône basin, France; Fig. 1a and b). The Bienne River is the most important tributary of the Ain River with an interannual average discharge of 29.3 m^3/s at the Jeurre gauging station (calculated with daily discharge over the 1971–2020 period, www.hydro.eaufrance.fr). The hydrological regime of the Bienne River is influenced by snow melt and rainfall, with significant fluctuations in river discharge. Monthly discharges are lowest in August and highest in March (10.7 and 43.1 m^3/s, respectively). During flood episodes, daily discharge can reach 270 m^3/s for a 2-year flood, 390 m^3/s for a 10-year flood, 490 m^3/s for a 50-year flood, and more than 600 m^3/s historical floods (e.g. up to 680 m^3/s for the flood of February 15, 1990).

Since the 19th century, river engineering has strongly modified the Bienne River system to improve navigation (historically for log driving and more recently for canoeing), protect human facilities, produce hydroelectricity, and facilitate gravel extractions (Janod, 1985; Bravard et al., 1998; Bravard, 1999). Today, 106 river flow obstacles are documented for the Bienne Basin (Fig. 1b, ROE database, www.data.gouv.fr). Spatial density of river infrastructures is similar in the upper and the lower parts of the Bienne basin with 0.3 and 0.4 low-head dams or sills per km of river straight, respectively. However, in the upper part, these obstacles are concentrated near and in the city of Morez (Hauts de Bienne municipality), while they are more dispersed in the lower part. Two large dams also influence the Bienne River flow: the Etables Dam (27 m), built between 1930 and 1932 downstream of the city of Saint-Claude and the Coiselet dam (37.5 m high), built across the Ain River between 1968 and 1970 which controls 2.6 km of the Bienne River level at its outlet (Fig. 1b). Considering the effect of dams, water levels are anthropogenically controlled on 14% of the river drop and 15% of the river course. Consequently, sedimentary transport in the Bienne River has been highly altered (Landon et al., 1998, 2000). With data from the monitoring of the river system since 1993 and given by the Haut-Jura Natural Park as the main stakeholder (www.parc-haut-jura.fr) predominant manifestations of these disturbances can be detailed as follows:

(i) a dramatic decrease in sediment transport from 25,000 to 8000 m^3/y since the 1950s,
(ii) a lack of more than 550,000 m^3 of riverbed sediments in the lower part of the river,
(iii) a deep incision of the riverbed, up to 2 m in some sections,
(iv) a channel narrowing of about 40% to 50%,
(v) an armoring of the stream over most of the river course (partially or totally over the channel width, depending on reaches).

These hydro-sedimentary issues also affect the Ain River downstream of the confluence (Marston et al., 1995; Piégay et al., 2008; Dufour and Piégay, 2010).

The population density of the Bienne Basin is low, with an average of 60 inhabitants/km² (www.insee.fr). The two most important populated areas are the Hauts-de-Bienne / Morbier area (approximately 7,700 inhabitants) and Saint-Claude (9,500 inhabitants, population in 2018, www.insee.fr). Many industries are historically present in the Bienne Basin as nail factories, wireworks, edge-tool factories, undercutting, polishing, coating, eyewear, watchmaking, plastic industries, etc. A total of 1032 industrial plants (historical and currently operating) are documented in this basin (Fig. 1b, BASIAS database, www.georisques.gouv.fr). Their distribution differed between the upper and lower parts of the basin. The density is 0.7 installations per km² in the upper basin, because industrial plants are mainly located in and around Morez (Hauts-de-Bienne, 33 installations per km² locally). In the lower basin, the density is generally higher with 1.9 installations per km², but they are more evenly distributed along the Bienne River straight and its tributaries.

Connections to wastewater treatment plants and water treatment improvements have been adopted since the late 1970s, and the activity of the most polluting industrial sites has largely decreased because of a strong decline in the local industry. However, contaminant levels are still high, and hotspots have been identified since the 1990s when the monitoring of metals in the Bienne River was initiated by the Haut-Jura Natural Park. The metals are mostly related to the non-controlled releases of industrial and urban sewage.

3. Material and methods

3.1. Sampling strategy

Along the Bienne River, six sampling stations were chosen at key locations to analyze spatial and temporal changes in metallic and organic contaminants (Fig. 1b and c; Supplementary material S.1). At stations 1 to 5, fine-grained sediments were sampled in riverbank during October and November 2018. Samples were collected across the erosional surfaces with a stainless-steel shovel according to the method described by Dhivert et al. (2016):

(i) When the riverbank was visually homogenous, sediments were sampled at vertical intervals of 20 cm.
(ii) When visual transitions occurred, each layer was sampled (minimum of 10 cm thick).

Station 1 was located downstream of Morez. At this place, the Bienne River is confined in deep gorge. The stream channel is steep (14‰ slope). The riverbed does not exceed 12 m wide. Sediments were sampled in a 140 cm high bank deposit (about 20 m long and 5 m wide), trapped in a channel widening in the right bank.

Station 2 was upstream the city of Saint Claude, where the Bienne River gorge became larger. Here, a floodplain has been developed over 2.2 km of the river course. Alongside the sampling site, overbanks are constrained (75 m wide maximum) by the bedrock in the left bank and embankments in the right bank. The slope of the stream channel is 6‰. The riverbed has considerably narrowed since the 1950s, from about 25 m to 15 m wide presently (www.remonterletemps.fr). Sediments were sampled over the thickness (150 cm) of a cut bank, between two meanders.

Station 3 was established in the left bank of the Etables reservoir, 40 m upstream of the dam. Here, fine-grained sediments have accumulated since the 1950s (at least), over 180 m in length and 40 to 60 m in width. Riverbank sediments were sampled during a maintenance period within the empty reservoir, where the sediment accumulation was the thickest (380 cm).

Station 4 was 4.3 km downstream of the Etables dam. Here, the valley become narrower over a 5 km long section. The slope of the stream channel is 4‰. The riverbed wide is about 20 m presently but

was about 25 m in the 1950s. Fine-grained sediments have settled in bank over a large part of this section. Sediments were sampled over the thickness (115 cm) of such depositional setting, in the right bank.

Station 5 was located 11.7 km downstream of the latter site, where the valley and the floodplain are larger. This station corresponds to a 390 m long section, relatively straight-lined and upstream a meander. Overbanks are constrained in a band of about 120 m wide maximum, limited by the bedrock in the left bank and a dyke in the right bank. Since 1970 a bridge crosses the river at this place and divides the floodplain with its structure. The stream channel slope is 4‰. The riverbed has narrowed from 60 m to 45 m wide since the 1950s. Samples were collected, in the right bank, 150 m downstream of the bridge, over the thickness of the riverbank (100 cm). Here, the river cut into a natural levee.

Station 6 was located at the river inflow to the Coiselet reservoir in the inner part of the meander between villages of Dortan and Chancia (Fig. 1b and c). At this place, a chute channel crosses the right bank, delimiting a vegetated island of 840 m long and 60 to 80 m wide. The stream channel slope is considerably lower than other stations (0.8 ‰), due to the influence of the Coiselet reservoir. Overbanks can reach 230 m wide maximum. This station has stabilized and aggraded since the 1950s, its history is detailed further to establish the age model (§ 4.2). Two sediment cores were collected, approximately 30 cm apart in the middle of this island on May 05, 2019, using a stainless-steel Russian corer. The first one captured the top 50 cm of sediments, and the second was a sedimentary sequence from 34 to 84 cm in depth. A 84 cm long master core was built in the field, using these two composite cores collected. Sediments layers were directly sampled in the field, at 4-cm intervals with a ceramic knife.

In addition, some sediments were sampled with a stainless auger at the base of a historical floodplain located 740 m downstream, above coarser sediments composed of gravels and cobbles (250-270 cm deep). This sample was collected to access concentrations of TE in old sediments. Actually, this former floodplain of 1.1 km long and 240 m wide maximum was settled on the left bank during the late 18th to early 19th centuries. Currently, the top of the floodplain is approximately 3 m above the water level regulated by the Coiselet Dam and can be related to a terrace functioning, with a lateral erosion of about 40 m between the 19th and the 1950s, and additional 10 m between the 1950s and 2020 (www.remonterletemps.ign.fr).

To prevent cross-contamination, all materials used for sampling were washed with HNO_3 (30%) and acetone prior to sample collections. Sediment slices were preserved at 5 °C in precleaned glass containers.

3.2. Analytical method

Grain size analyses were performed on fresh sediment samples with a Malvern Mastersizer 3000 laser diffraction microgranulometer, after a 30 s ultrasonic step (analyzed particles ranged between 0.01 and 2000 µm, Supplementary material S.2). Organic debris, such as leaves and wood fragments, present in some slices, were manually removed before analysis. The median grain-size (D_{50}), ten and ninety percentiles (D_{10} and D_{90}), cumulative volumetric percentage of fine-grained sediments (<63 µm), clays (<2 µm), silts (2–63 µm), and sand (63–2000 µm) were computed using the geometric method of Folk and Ward (1957).

An age model was proposed for the sedimentary core sampled at station 6. It was based on the calculation of sedimentation rates between temporal markers at different depths in the sedimentary deposits. The top of the core was assigned the date of the last flood event before the sampling date

(during the winter of 2018-2019). We used temporal markers related to the ^{137}Cs activity profile and grain-size transitions throughout the core to detail the age model (Supplementary material S.2). The artificial radionuclide ^{137}Cs has been present in the environment since the beginning of atmospheric nuclear weapon testing in the early 1950s. Two events can be identified in the Jura Mountains:

(i) the maximum ^{137}Cs atmospheric fallout in 1963 (coming from the peak of nuclear weapon tests, NWT, prior to the international moratorium), and
(ii) the 1986 fallout peak following the Chernobyl Nuclear Power Plant Disaster (C-NPPD; Meusburger et al., 2020; Foucher et al., 2021).

In this study, radiometric analyses were performed using the analytical service of the Institut de Radioprotection et de Sureté Nucléaire (IRSN/PSE-ENV/SAME, Veniset, France, www.irsn.fr). The samples were composed of approximately 50 g of dry sediment (< 2 mm) packed in air-tight plastic boxes for a 24-h gamma counting with very low-background detectors used for gamma spectrometry (coaxial HP Ge N-types). The laboratory detected ^{137}Cs with an energy peak at 661 keV in the spectrum area free of interference. The activities were corrected to the time of the collection period. Measurement uncertainties were approximately 2.5% with a detection limit between 0.7 and 2.4 Bq/kg.

For each sample, a part of the material was dried at 40 °C for 48 h. TEs analyzes were performed on sieved sediments through a 63 µm disposable nylon mesh in order to normalize the data and limit the grain-size influence on metal concentrations (Horowitz and Elrick, 1987). In addition, the DEHP and indicator PCBs were also analyzed in the < 2 mm fraction of riverbank sediments (Supplementary material S.2).

Geochemical analyses were performed using the analytical service of Eurofins Scientific (Saverne, France, www.eurofins.fr) with standardized procedures NF EN ISO 17294-2 and 13346 for TEs and XP X33-012 and CEN/TS 16183 for organic contaminants (www.afnor.org).

Concerning TEs, sieved materials were digested using an *aqua regia* procedure and TEs were analyzed by mass spectrometry (ICP-MS), except for Hg which was analyzed by cold vapor atomic absorption spectrometry (CV-AAS) (Tab. 1). All digestion processes and analyses were qualitatively checked by analyses of internal reference materials (z-score ranging between -1.2 and 1.05).

In this study, enrichment factors (EF) were calculated to evaluate TE contaminant levels. The normalization procedure performed in our study was described in Grosbois et al. (2012) and references therein. The local geochemical background used to calculate EF has been defined in the old sedimentary level sampled at the base of the former floodplain downstream of the station 6 (see § 3.1.). This sediment layer gave non-impacted concentrations ranging in the same intervals compared with preindustrial concentrations analyzed in other basins of metropolitan France (Tab. 2).

Concerning the DEHP and PCBs, solid-liquid extractions with low temperature purifications were done before analysis using gas chromatography / mass spectrometry (GC-MS, Tab. 1).

4. Results and discussion

4.1. Grain size variations and history of the river management

The samples are chiefly composed of fine-grained sands and silts (Fig. 2). At some stations (2, 3, 5, and 6), sedimentary profiles are interspersed with layers richer in organic-rich layers and/or medium to coarse sands. Different grain size groups can be defined according to the percentage of the <63

µm fraction, as well as silts and clays proportions (Fig. 2). They are described below from the coarsest to the finest grained groups:

- In group 1, the average percentage of the <63 µm fraction is 26.1% (range: 9.0% - 41.9%), with less than 0.3% of clays (<2 µm fraction). This group has a high average percentage of sand (63–2000 µm fraction) of about 73.8% (57.9–91.0%). The D_{10}, D_{50}, and D_{90} grain size parameters averaged 25 µm (8–70 µm), 144 µm (81–291 µm), and 535 µm (239–1390 µm), respectively. This grain size group corresponds to all samples of stations 1, 4, and 5; to layers between 0 and 110 cm in depth at station 2(the unit U2.1); and to sedimentary layers between 52 and 84 cm in depth at station 6 (the unit U6.2). At the base of the sedimentary core sampled at station 6, the D_{90} parameter differs from the 52–68 cm sequence with a mean value of 269 µm (239–294 µm) while the 68–84 cm sequence presents higher values (mean of 527 µm, 309–915 µm). This basal sequence appears to be reworked and contains layers enriched in coarse sands.
- The group 2 has a larger fraction of fine particles (<63 µm), with 54.7% on average (43.1–64.1%). Average percentages of silts and sands are52.8% (41.0–61.5%) and 45.8% (35.9–56.9%), respectively. Clays are present in a proportion of 1.5% on average (0.5–2.6%). On average, grain size parameters present mean values of 6 µm (5–9 µm) for D_{10}, 55 µm (37–73 µm) for D_{50}, and 209 µm (155–271 µm) for D_{90}. This group corresponds to the upper sedimentary units sampled at stations 3 (U3.1 between 0 and 260 cm in depth) and 6 (U6.1 between 0 and 52 cm in depth).
- In group 3, the <63 µm fraction is much higher than the other groups, with a mean value of 83.0% (77.2–92.2%). This sedimentary group is mostly composed of silts with an average value of 79.3% (74.1–86.8%), while clays account for 3.7% on average (3.1–5.5%). It contains less sand than the other groups, (ca. 17.0% on average, 7.8–22.8%). The grain size parameters are also finer, with averages of 4 µm (3–5 µm), 21 µm (10–36 µm), and 86 µm (56–97 µm) for D_{10}, D_{50}, and D_{90}, respectively. This group corresponds to the deepest layers at stations 2 (U2.2 between 110 and150 cm in depth) and 3 (U3.2 between 260 and380 cm in depth).

These three grain size groups can be related to different deposition mechanisms. The group 1 is mostly unimodal and well sorted, composed of fine-grained sands and silts (Supplementary material S.3). These sediments are typically transported in the suspended load, in slope and specific stream power conditions of the Bienne River (1.8 to 3.6 10^2 N/m² according to Dade and Friend, 1998; Kleinhans and van den Berg, 2011). Groups 2 and 3 are richer in clays and silts and moderately to poorly sorted. Such sediments are deposited under low velocity flow conditions, fostering the settling of the wash load. Both stations 3 and 6 are presently influenced by the Etables and Coiselet dams. Changes in the wash load sedimentation capacity should be related to changes in the water level management. However, there is no readily available information related to historical water level management of these dams. The base of the riverbank at station 2 (U2.2) is also composed of fine-grained sediments (group 3), but this deposit was probably caused by temporary fishing structures (wire-wrapped dams) installed between 1961 and 1965 for fish farming. This information is documented in the historical records of the Jura Department (ref. 2517 W 120, www.archives39.fr). After the removal of these river flow obstacles, the upper unit of the riverbank (U2.1) was deposited under a higher flow energy (shift from group 3 to group 1). Evidence of a post-1950s deposition is also given in § 4.2.

Bienne riverbanks were deposited on basal coarse sediments composed of medium to coarse sands, gravels, cobbles, and boulders (Fig. 1c). These coarse sediments were manually measured in station

1, 4 and 5. Grain size parameters are close between these stations and similar to sediments presently transporting in the bedload, with on average D_{10} = 6.1 cm (5.0–6.8 cm), D_{50} = 11.2 cm (10.8–11.9 cm), and D_{90} = 20.9 cm (18.8–24.2 cm; n=90). They correspond to the former riverbed now covered by finer sediments belonging to the riverbanks. Aerial photographs from the 1950s show different fluvial styles for the Bienne River compared to present day (www.remonterletemps.ign.fr). Bed material was visually more abundant at that time and the riverbed was wider and moderately braided in the lower section (Supplementary material S.4). Alternate bars were present in the upper section. These patterns are typical in confined and partly confined valleys as the Upper and the Lower Bienne River (Fryirs, 2013, 2017; O'Brien et al., 2017). The riverbed grain size and the specific potential stream power of the Bienne River are in concordance with a moderately braided channel pattern (Kleinhans and van den Berg, 2011). The sharp grain size transition between coarse and fine-grained sedimentary deposits reflects morphological changes of the Bienne riverbed which have occurred since the 1950s. It indicates an important drop of the bedload transport and a change in hydro-sedimentary processes fostering the settling of sediments transported in the suspension over the former active channel. It is consistent with the definition of infrastructure-induced legacy sediments proposed by Vauclin et al. (2020b). According to the Lane's balance (Lane, 1955), an equilibrium is maintained between water discharge, slope, sediment load and grain size. Changes in any of these parameters lead to changes in the others and drive channel adjustments. In coarse-bedded rivers, dams (even low-head dams) can largely influence the channel morphology by impacting the slope, the sedimentary transport and grain size distribution upstream and downstream of the infrastructures (Casserly et al., 2020; Brenna et al., 2020). They can also influence the spatial and temporal dynamics of suspended sediments (Casserly et al., 2021). In addition, coarse sediment delivery by the Bienne River has been dramatically reduced by many infrastructures built on slopes and embankments to limit river wandering since the middle of the 20th century. Consequently, some river sections have been partially or totally disconnected to supply reservoirs of coarse sediments. River engineering has resulted in a deep loss of sediment connectivity at the catchment scale (Borselli et al., 2008; Najafi et al., 2021). Fine-grained deposits have been the consequence of an important change of the riverbed functioning as a narrowing and a stabilization process of the active channel, accompanying by an incising of the wetted channel. Such evolutions follow stream anthropogenic disturbances as slopes tiering and the bedload starvation (Marren et al., 2014; Provansal et al., 2014; Fencl et al., 2015).

4.2. Age of the riverbank formation

In the sediment core collected at station 6, ^{137}Cs activity results attest to a post-1950 deposition with a minimum of 2.9 ±0.8 Bq/kg at the base of the core (Fig. 3). The ^{137}Cs vertical profile shows a well-defined peak at a depth of 48–52 cm (17.3 ±2.4 Bq/kg). No ^{241}Am was detected, and this shape of the ^{137}Cs profile was in good agreement with the C-NPPD in 1986.

The grain-size transitions recorded in this core (Fig. 2: station 6) can provide additional time markers associated with morphological changes documented in historical data (www.remonterletemps.ign.fr). Aerial photographs for the Station 6 area are available since 1953. From 1953 to 1969, this area was a point bar, which is characteristic of the inner curve of meanders. The aerial photograph from 1971 (end of the first filling period for the Coiselet reservoir, Fig. 1) shows a cleared area, partly flooded. The sedimentary pattern of the 68–84 cm sequence (down to the layer composed of pebbles and cobbles representing the base of the bank) is a discontinuous record. The 68–72 cm interval reflects sediment remixing during the reservoir-filling period and/or flood deposits during that time (Dhivert et al., 2015a). In addition, several flood events occurred during the Coiselet Reservoir building period (Paravy and Fournevy, 1973). Consequently, unit U6.2 is

dated with low accuracy as being deposited during or before reservoir filling (before 1971 but after 1950) as erosional episodes could have occurred during the deposition of this unit (Fig. 3).

Aerial photographs of the station 6 area from 1975 to 1984 show the presence of scroll and chute bars with mostly light-colored deposits (probably enriched in sand). A sparse vegetation developed at the top of bars attesting to their stabilization. In more recent photographs, from 1989 to 2018, bars were well stabilized and connected each other by a dense vegetation. Deposits were also considerably darker. Riparian vegetation can play a key role in the stabilization of river bars and in the trapping of the suspended load (Rodrigues et al., 2007; Wintenberger et al., 2015; Jourdain et al., 2020). This process continues to operate in some reaches of the Lower Bienne River. This morphological change occurred during the C-NPPD fallouts and is consistent with the ^{137}Cs peak between units U6.1 and U6.2. It attests to a decrease of the transport energy at this time (Fig. 3, grain size groups 2 and 1 respectively in Fig. 2). These morphological and sedimentary changes could also be fostered by an evolution of the reservoir impoundment (see § 4.1). The base of the sedimentary sequence (64–68 cm) can be dated to 1975 ±2 year. according to a constant sedimentation rate (1.5 cm/year) based on the thickness of the sampled slices and bounded by the ^{137}Cs peak and by the influence of the Coiselet reservoir. To refine the age model, the age of this sedimentary level can be constrained to 1971 (i.e. the end of the filling period of the dam). Under this other scenario, the sedimentation rate of the 52–68 cm sequence was 1.1 cm/year. Age models are similar between these two scenarios, with uncertainties only extending to 4 year (Fig. 3).

The ^{137}Cs was not analyzed in riverbank sediments at upstream stations (1 to 5). Indeed, the sampling strategy with riverbanks was not suitable to robustly identify and characterized ^{137}Cs peaks. However, we used other specific markers of the Anthropocene to assess the relative age control of riverbanks sediments such as the DEHP). It was the first phthalate ester introduced as a plasticizer in the 1930s for PVC (polyvinyl chloride) fabrication (Graham, 1973). By the 1950s, the PVC production and consumption marked a real takeoff (Mulder and Knot, 2001). Nowadays, DEHP has become the most widely used plasticizer (Jamarani et al, 2018). This compound is ubiquitous in the environment and can accumulate and be preserved over long time in sediments (Bergé et al, 2013; Goa and Wen, 2016). DEHP is quantified in all sediment layers collected in riverbank (station 1 to 5) and in the core (station 6), ranging between 24 and 870 µg/kg (Fig. 4). During the sediment collection, plastic debris in association with other various wastes were also visible all over the height of banks. PCBs can also be considered as chemostratigraphic marker of the Anthropocene (Gałuszka et al, 2020; Dong et al, 2021). PCBs are detected in all stations of the Bienne River, the sum of 7 indicator PCBs ranging between < 1 and 19.5 µg/kg (Fig. 4).

All these indicators, in addition to the ^{137}Cs dating of the core, represent robust arguments to consider the deposition of the Bienne riverbanks during the second part of the 20th century, concurrent with the building of several dams, sills, and embankments during this period. This interpretation is also consistent with observations (aerial photograph survey) of riverbed narrowing since the 1950s.

4.3. Temporal evolution of contaminants recorded in stored sediments

In the Bienne riverbanks, the highest TE enrichments occur in sediments from the most upstream station 1(Fig. 5, Tab. 3). Here, high contaminant levels (EF ≥ 10) are registered for Cu (EF ranges between 20.4 and 25.8), Pb (10.9–25.0), and Sn (15.5–34.5) in all layers; and Hg between 30 and 110 cm (11.1–12.7). Moderate enrichments (5 ≤ EF < 10) are calculated for Ag (7.2) and Hg (9.5) in separate layers (120-140 cm and 0-20 cm layers respectively) and Zn except at the base of the sampled column (6.1–7.3). Low enrichments (2 ≤ EF < 5) are calculated for most of the analyzed samples for Ag between 0 and 110 cm (ranges: 3.1–4.6), As (ranges: 2.0–2.2), Bi (2.5–3.6), Ni (2.0–

2.7), Sb (2.7–4.8); more rarely for Cd (2.3) and Zn (4.8) both in the 120-140 cm layer. A decreasing trend can be recognized for Ag from the base to the top of the riverbank and for Cu, Hg and Pb from the 90-100 cm layer to the top. Concerning organic compounds, the highest values are reached in the 120-140 cm layer with 850 µg/kg for DEHP and 19.5 µg/kg the sum of 7 indicators PCBs (Fig. 4). In other layers, concentrations range between 24 and 66 µg/kg for the DEHP and are < 1 µg/kg for all PCB congeners.

At station 2, the most enriched TEs are Cu (6.0–8.1) and Sn (5.1–11.3). However, it presents moderate EF values compared to upstream, except for Sn in the 30–50 cm layer (high enrichment). Moderate enrichments are also calculated for Bi (6.7–7.5), Hg (5.0), and Pb (5.0) in some layers. Low enrichments are recorded for Zn (2.2–3.6) across the entire column; Hg (2.2–3.7), Ni (2.1–2.5), and Pb (2.5–4.1) in most of the analyzed samples; along with Ag (2.0) and Cd (2.3) in separate, single layers (140-150 cm and 30-50 cm respectively). The highest DEHP concentrations are analyzed in layers between 80 and 150 cm (570-870 µg/kg). Other layers (form the top to 50 cm) range between 290 and 360 µg/kg. The sum of PCBs decreases from 14.1 to 6.6 µg/kg form the base to the 80-100 cm layer. A maximum of 18.5 µg/kg is reached in the 30-50 cm layer before to return to 5 µg/kg in the top layer.

At station 3, TE enrichments are even lower than at stations 1 and 2. High and moderate contaminant levels are only recorded for Bi (6.6-11.3), Pb (5.7), and Sn (5.2) between 0 and 260 cm. Low enrichments are calculated in most layers for Bi (2.9–3.4), Cu (2.8–3.6), Hg (2.8–3.9), Pb (2.6–4.3), Sn (2.1-4.5) and Zn (2.3–2.6); and in a few samples for Cd (2.0–2.3) and Sb (2.2-3.5). DEHP concentrations are stronger in layers between 0 and 140 cm (250-850 µg/kg) than in other layers between 185 and 380 cm (34-130 µg/kg). The sum of PCBs ranges between 4 and 6.9 µg/kg in 0-140 cm layers, whereas all PCBs congeners are < 1 µg/kg in other layers.

TE Enrichments are slightly higher at station 4 than at station 3. Moderate to high enrichments of TEs are noted in three sampled layers between 60 and 115 cm for Bi (5.1–22.4), Cu (5.2–5.4), Hg (15.7), and Pb (9.5–11.9); and in all samples for Sn (6.1–12.5). Low enrichments are also calculated for Ag (2.9–3.3), Bi (2.1–4.9), Cd (2.1–2.8), Cu (2.5–4.4), Hg (2.4–4.6), Pb (2.4–4.1), Zn (2.9–3.9); and in a few samples for As (2.0), Ni (2.3), and Sb (2.4–3.4). A decreasing trend can be identified for Bi, Pb and Zn from the 80-100 cm layer to the top. In this station, DEHP concentrations increase from the base to the 30-50 cm layer (57-470 µg/kg). In the top layer, the DEHP concentration is slightly lower (320 µg/kg). Concerning the sum of PCBs concentrations range between 2.5 and 17.3 µg/kg except for the 30-50 cm layers where all PCBs congeners are < 1 µg/kg.

TE enrichments are similar at stations 5 and 6. At station 5, moderate contaminant levels are calculated for Hg (5.7) in the 10–20 cm layer and Sn (5.0–5.9) between 10 and 60 cm. Low enrichments are recorded for Cu (2.1–2.6), Pb (2.0–2.7); Ag (2.1), Bi (2.1), Hg (4.9), Sn (3.9–4.7) and Zn (2.0-2.1). At station 6, some layers also present moderate Sn enrichments (5.3–6.7), while the other samples show low enrichments (2.5–4.7). Bi is slightly enriched from the base of the core, rising until sedimentary levels settled during the 1990s (2.3–3.3). Sediments deposited during the 2000–2010 period have negligible Bi enrichment. Low enrichments are also calculated for Cu (2.0–2.9) since the early 1970s, Pb (2.1–2.9) in all layers of the sampled sedimentary column, and Zn (2.0–2.2) only from layers deposited during the 1970s. Thus, a weak temporal mitigation of TE enrichments is recorded in this sedimentary core (Supplementary material S.5). Average EF decrease from the 1970s to the 2010s (from 3.1 to 1.7 for Bi, from 2.6 to 2.2 for Cu, from 2.9 to 2.2 for Pb, and from 2.1 to 1.6 for Zn). Sn reveals no temporal trend across the recorded period (3.5–3.9). Negligible enrichments (EF <2) are also detected in all the analyzed samples at each station for Cr (EF <1.9), Mo (EF <1.8), and W (EF <1.5). The temporal trend recorded in sediments of the Bienne River for most of

historical TEs is commonly recorded in Western Europe basins, following the improvement of wastewater treatments, local applications of the UE Water Framework Directive and changes in the urban and industrial development (e.g. Dendievel et al, 2022).

Concerning organic contaminants, DEHP concentrations range between 340 and 530 µg/kg in 70-100 cm layers and between 260 and 270 µg/kg in 0-40 cm layers of the station 5. In the sedimentary core of the station 6, DEHP concentrations are a bit lower. They fluctuate between 30 and 190 µk/kg from the 1970s to 2000s, with decade averages between 89 and 157 µg/kg. Concentrations range between 30 and 120 µg/kg in the 2010s with an average of 68 µg/kg. Several studies reveal that DEHP signal in sediments has considerably increased since the 1970s, in relation with the plastic production (Peterson and Freeman, 1982; Li et al, 2021; Kim et al, 2021). In Western Europe, sediment contaminations have begun to decrease since the late 2000s because of its regulation in the Environmental Quality Standards Directive of the EU Water Framework Directive as a priority substance (European Council, 2008; Nagorka and Koschorreck, 2020). The temporal evolution recorded in the Bienne River core is consistent with the production and regulation history explained above.

The sum of PCBs varies between 3.2 and 3.7 in layers collected in the station 5, except for the 0-10 cm and the 30-40 cm layers where all PCBs congeners are < 1 µg/kg. In the station 6, recorded PCBs concentrations are at maximum at the end of the 1970s (15.7 µg/kg), before to sharply decrease and reach lower values since the end of the 1990s (3.2-5.5 µg/kg; Supplementary Material S.6). Such temporal evolution is typically recorded in Western Europe basins. It occurred synchronically with a drop of global emission following the application of a regulation which prohibited the use of PCBs in open environments (Breivik et al, 2002a, b, 2007; Dendievel et al, 2020a).

4.4. Spatial evolution of riverbank contaminations along the river course

In riverbank sediments of the Bienne River, contamination levels are high for TEs, especially in the upper reach. The highest TE enrichments in all Bienne riverbanks across the river course are recorded for Cu, Pb, Sn, Hg and Zn. Strong correlations are calculated between Cu, Pb, Sn and Zn enrichments ($r > 0.94$. $p < 0.05$, $n = 47$). There are also weak but significant correlations with As, Ag, Hg, and Sb (r between 0.64 and 0.82, $p < 0.05$). TEs such as Cu, Hg, Pb, Sn, Sb, and Zn are commonly enriched in basins draining land with metal industries (Ettler et al., 2005; Jasminka and Robert, 2011; Grygar et al., 2012). In the Bienne basin, known sources were nail factories, wireworks, edge-tool factories for all cited TEs, undercutting, polishing, coating especially for Cu, Pb, Sn and Zn (www.parc-haut-jura.fr). Downstream of the station 1, EFs show an important gradient from high to low contaminant levels (e.g.r Cu, Fig. 6). Specifically, the Cu EF decreases sharply in the Upper Bienne River (stations 1 and 2). However, in the Lower Bienne River (stations 3 to 6), enrichments are lower with slight variation between stations. Another hot spot influence is marked for elevated Bi concentrations at stations 3 and 4 (Fig. 6). Other TEs are also concerned as Hg, Pb and Sn but in a lesser extent than Bi. Several plastic industries are located near these stations. They mainly bismuth vanadate for plastic coloring and as bismuth alloys for mold making (Ojebuoboh, 1992; Kus et al., 2013). A quick EF decline is also recorded for Bi downstream of this pollution hotspot. Furthermore, DEHP and PCB concentrations in the Bienne riverbanks are relatively ubiquitous compared with neighborhood basins (Net et al, 2015; Dendievel et al, 2020a). Because of their wide use in different applications, DEHP and PCB sources are numerous and widespread in basins. In this context, their river course profiles do not show clearly identified pollution hotspots.

At the catchment scale, the sedimentary cascade controls the fate of river sediments, as described by Burt and Allison (2010). This cascade has spatial and temporal imprints on sediment geochemistry, influencing the spread and weathering of TE-bearing particles (Lecce and Pavlowsky, 2014; Dhivert et

al., 2016; Ledieu et al., 2020). In mountain rivers, the spreading of contaminant particles could be enhanced with steep slopes and intense hydro-sedimentary dynamics related to the functioning of coarse bedded streams. However, this study in the Bienne River reveals a strong spatial attenuation of Bi, Cu, Hg, Pb, Sn and Zn enrichments (also for Ag, As and Sb but enrichments are lower), attesting to an extremely slow transport of sedimentary contaminants in the downstream direction. The important alteration of the sedimentary transport capacity and the strong storage capacity of fine-grained sediments in banks (c.f. § 4.1) have been followed by a rapid capture of contaminant particles downstream of their sources. The Spatial Attenuation ($SA_{1/2}$) of Cu and Bi was appreciated along the Bienne River course as the distance necessary to decrease enrichments by a factor 2 downstream of peaks ($SA_{1/2}$ = 12 km for Cu and 8 km for Bi, Fig. 6). Close values (about 10 km) can be calculated with TE contaminations of floodplain and stream sediments in other similar rivers, downstream of mining and manufacturing facilities (Pizzuto, 2014; Lecce and Pavlowsky, 2014; Pavlowsky et al., 2017). Authors also explained the slow transport of contaminated particles by a strong storage in the floodplain.Therefore, in these conditions, depending on river flow rates, the alteration of the bedload transport, and the intrinsic properties of stored sediments, riverbanks can establish only temporary sinks for contaminant particles in the sedimentary cascade. These stored particles can be released during erosional episodes (Förstner, 2004; Coynel et al., 2007; Reis et al., 2014; Dhivert et al., 2015a). This is the case for the Bienne River, where evidence of bank erosion is visible along the river course. Erosion is particularly noticeable at the base of riverbanks where non-cohesive sediments are strongly eroded in some reaches (Fig. 1c). In the Bienne River, these erosion patterns have been described since the early 2000s (Landon et al., 2000). This can be explained by disturbances in the sedimentary transport, leading to lateral erosion of bank sediments because the vertical incision of riverbed sediments is advanced (Lyons et al., 2015). These results highlight the key role of sedimentary cascade inefficiency in the spatial and temporal trends of contaminants.

4.5. Spatial and temporal influence of trace element sources

To explain the strong decrease in TE enrichments along the river, we intended to quantify the provenance of sedimentary contaminants recorded in the core sampled at the river outlet. For this purpose, we applied the fingerprinting procedure defined in the FingerPro R package (Lizaga et al., 2018, 2020; Gaspar et al., 2019). In this approach, all the samples from stations 1 to 5 were considered as potential sources and those of station 6 were considered as a mixture of these sediments. We integrated the normalized TE-Al ratio dataset for the most enriched TEs (Bi, Cu, Hg, Pb, Sn, and Zn with EF >5, c.f. §4.3).

The first step of this procedure consists in identifying which geochemical tracers are the most discriminant to characterize anthropogenic sources. To this end, a stepwise multivariate discriminant function analysis (DFA) was used to determine the TE-Al ratio, which passed a nonparametric Kruskal-Wallis H test. In our dataset, Hg, Bi, and Sn were excluded with this procedure ($p > 0.05$). The second step corresponds to multivariate linear discriminant analysis (LDA) performed with the remaining tracers (Cu, Pb, and Zn). This procedure allows the clustering of three well-defined endmembers as samples of station 1, station 2, and a group composed of all samples from stations 3, 4, and 5 (Fig. 7a). These results are consistent with the spatial distribution of the EF defined in Section 4.3. In the last step of this procedure, a standard multivariate mixing model was used to calculate the geochemical fingerprinting index quantifying the relative weights of these three endmembers in the composition of the mixture sediments (sedimentary core from station 6; Fig. 7b).

Endmember 3 is largely dominant in the composition of mixture sediments, weighing between 94.4 ±5.4% and 98.3 ±1.9% (±1δ). Endmember 2 represents between 1.6 ±1.9% and 5.4 ±5.4% of the

mixing pattern, and endmember 1 is limited (≤0.2 ±0.2%). The goodness of fit (GOF, Collins et al., 1997) coefficient ranges between 89.7% and 94.4%.

Enrichments are the highest in the upper part of the river (stations 1 and 2). While sources are more concentrated in this upper reach, they have little influence on the geochemical composition of sediments in the lower river (stations 3 to 5) and in the mixed sediments at station 6. In the sediment core sampled at the river outlet, contributions from temporal changes of the three endmembers are recorded in the sediment sample assemblages (Fig. 7b). The sum of endmembers 1 and 2 is low but presented a notable temporal variability. Indeed, the influence of the upper river reaches a maximum during the 1970s, with a mean value of 4.5% (2.5–5.5%), before decreasing until the 1990s, when it averages 2.2% (2.1–2.3%). During the early 2000s, this contribution become more important. Then, it reaches a relative weight of 2.9% (1.7–4.1%) in the 2010s.

These results in space and time are clearly related to the low capacity for transport of contaminant particles in relation to the alteration of the sedimentary cascade (§ 4.3). This resulted in contaminant particles being stored in riverbanks and upstream infrastructures. This phenomenon can be heterogeneous at a basin scale, and TE-bearing particles can be transported more easily in certain reaches than others. The alteration of sediment transport is particularly strong in the upper Bienne River, where the bedload is most lacking. The situation is relatively less critical in the lower river straight because certain tributaries continue to provide sediments (Haut-Jura Natural Park, personal communication). This explains the weak connectivity between the upper and lower basin. A better-consistent bedload supply in the lower basin by functional tributaries improves the sediment connectivity in this section. Furthermore, it probably contributes to a dilution of sedimentary contamination coming from the upper reach and/or an important alteration of the upstream geochemical signature along the river course. Under these conditions, the geochemical imprint of sources located in the lower part of the basin became relatively more inflowing. The spatial distribution of sources probably also played a key role. Industrial plants are more localized in the upper part of the Bienne basin and are more evenly distributed in the lower part (Fig. 1; §2). The recent magnification of the upstream signal recorded in the core may be related to the increase of bank erosion process, described since the 2000s (see § 2).

4.6. Implications of this study

Since the implementation of the European Water Framework Directive, many efforts have been focused on improving the inclusion of sediment issues in river basin management plans (www.sednet.org; Brils, 2020). Our study provides relevant findings for this purpose by highlighting the relationships between sediment dynamics and long-term water quality at the river scale.

From a methodological point of view, this study highlights the possibility of sedimentary contaminants being trapped in mountain rivers as a result of disturbances of sedimentary transport. Innately, it may be difficult to spot deposition sites in mountain rivers because of high flow velocities, heavy hydro-sedimentary dynamics, and relatively narrow floodplains. In this study, we highlight significant storage of contaminated sediments in riverbanks. In these conditions, this study reveals an important downstream decrease in sedimentary contamination. TE enrichments at the river outlet do not represent an average TEs distribution at the basin scale. Contaminant sources in the upper part have a low influence on the geochemical composition of sediments in the lower part, even a few kilometers downstream. While the contribution of the upper river reach is low in the composite sediment of the downstream core, a temporal change is recorded. Concerning organic contaminants, because of numerous and widespread sources, any clear pollution hotspot can be identified along the river course. For both metallic and organic contaminants, source influences are spatially limited along the river course. Such spatial and temporal influences of sources, driven by changes of the

sediment connectivity between river sections can have deep implications for source monitoring in river basins.

The question of the longitudinal influence of downstream sources is generally studied from various standpoints:

(i) The mobility of contaminants related to chemical and physical properties of their bearing phases during the sedimentary cascade (Bossy et al., 2010; Dhivert et al., 2016; Grosbois and Courtin-Nomade, 2019).
(ii) The influence of hydro-sedimentary events like major flood events as a dilution process or reactivation of old but important contamination sources (Coynel et al., 2007; Bábek et al., 2011; Dhivert et al., 2015a).
(iii) The influence of dams on the dispersion of sedimentary contaminants (Vukovic et al., 2014; Frémion et al., 2016; Grygar et al., 2018; Zhu et al., 2019).

This study proposes a complementary approach by considering the long-term influence of hydro-sedimentary dysfunction on the river-scale transport of sediments and associated contaminants. A river course approach, as performed in this study, can be a solution to better evaluate the heterogeneity of environmental conditions and complex interactions with regard to the sediment transfer between river sections.

From a river functioning point of view, our study emphasizes the issue of legacy sediment management in mountain rivers. Geochemical analyses of Bienne riverbank sediments highlight elevated TE contaminations in the upper river. Here, enrichments are of the same order of magnitude as sediments settled during the enrichment maxima periods (1950–1980) in nearby large basins (Middelkoop, 2000; Ferrand et al., 2012; Grosbois et al., 2012; Dhivert et al., 2016; Dendievel et al., 2020b). This study agrees with other examples dealing with strong historical pollution in relatively small river systems at the head of larger basins, which are also impacted by previous human activities such as mining and associated smelting (Audry et al., 2004; Ettler et al., 2006; Resongles et al., 2014, Courtin-Nomade et al, 2016). Such high contaminant levels are less documented in industrial valleys such as the Bienne River, which drains various well-established manufacturing sectors. However, this situation is relatively common in European mountains. In many valleys, easy access to hydropower energy has fostered the development of diversified industrial networks persistent over long periods (Chabert, 1978; Ogilvie, 1993; Parrinello, 2018).

Since the early 2000s, erosion of the Bienne riverbanks has been magnified, releasing sediments and contaminants into the river. This newly available stock of pollutants in the riverbank sediment reservoir represents a threat to freshwater ecosystems. Compared to sediment quality guidelines provided by de Deckere et al. (2011), Cu, Hg, Pb, Sn, and Zn concentrations were higher than the lowest consensus-based level at all stations (indicating a poor ecological status). Moreover, Cu, Pb, and Sn concentrations exceeded the highest consensus-based level in the upper reach (attesting to potential toxic effects). For most western European basins, a resilience trajectory of contaminants has been tracked for decades because of strong declines in source releases. In this context, the erosion of legacy sediments can constitute active non-point sources that significantly impact water quality (Dhivert et al., 2015; Donovan et al., 2015; Pavlowsky et al., 2017; Jiang et al., 2020). This erosional process is expected to intensify over the 21st century with hydroclimatic changes and their associated increase in the frequency and intensity of extreme flood events, modifications of land cover and sediment delivery, and entrainments (Lane et al., 2007; Szalińska et al., 2020; Pirkhoffer et al., 2021).

Mitigation efforts to limit legacy sediment erosion (at least in hotspots) can be an effective approach to improve or limit the degradation of water quality (Fleming et al., 2019; Noe et al., 2020; McMahon et al., 2021). From this perspective, understanding the long-term relationships between alteration of sediment transport and water quality, as has been done in this study, can provide strategic information to guide river restoration programs. In the case of the Bienne River, the settling capacity of fine-grained and contaminated particles was modified along the river straight because of human-made obstacles impacting the slope, river flow velocity, and supply/transport of coarse sediments. Restoring bedload transport can be a long-term solution to limit the storage of contaminated sediments and legacy sediment erosion.

5. Conclusion

This case study along the Bienne River exhibited a temporal and spatial distribution of legacy sediments that can be affected by strong hydro-sedimentary dysfunction at the basin scale. Other studies have rarely taken this basin-scale approach. Sedimentological and geochemical compositions of riverbank sediments attested to the deposition of relatively fine-grained legacy sediments in riverbanks since the middle of the 20th century. This sedimentary storage in the former active channel is a response to a huge depletion of the bedload transport and the slope tiering induced by river engineering. The Bienne River provides a good example of the long-term consequences of human-induced changes in hydro-sedimentary processes on coarse bedded and armored river systems. Consequently, important reservoirs of contaminants have been stored in Bienne riverbanks and may pose a significant threat to the freshwater ecosystem over the 21st century.

Considering a gradient of anthropogenic pressures at a basin scale, mountain rivers are generally considered as better preserved and are usually intended to play a role of biological reservoirs in large river basins. There is much interest in developing research projects involving stakeholders to better understand the legacy impacts of human activities and the fate of contaminant stocks regarding local hydro-sedimentary and hydroclimatic issues. Such studies can provide data to improve survey planning and assist in the re-evaluation of ecological refuges consistent with environmental protection of sensitive species.

These results also highlighted issues related to the long-term spread of sedimentary contaminants in relation to disturbances of the sedimentary transport. They also questioned the representativeness of recorded geochemical signals at the river outlet to basin scale TE contamination, at least in the context of strong disturbances of hydro-sedimentary processes. More studies in other basins will help to better understand this question.

Credit authorship contribution statement

Elie Dhivert: Conceptualization, Methodology, Investigation, Formal analyses, Writing – Review and Editing. **André-Marie Dendievel**: Validation, Writing – Review and Editing**. Marc Desmet**: Validation, Writing – Review, and Editing. **Bertrand Devillers**: Conceptualization, methodology, and funding acquisition. **Cecile Grosbois**: Validation, Writing – Review, and Editing.

Declaration of competing interest

The authors declare that they have no known competing monetary interests or personal relationships that could have influenced the work reported in this paper.

Acknowledgments:

This research program received financial and technical support from many stakeholders engaged in the preservation of the Bienne Basin: the Haut-Jura Natural Park, the Bourgogne-France-Comté region, the Rhône-Méditerranée-Corse Water Agency, the Jura Department, the Saône-Doubs local public basin establishment, fishing federations of the Jura and national, and the speleology club of Saint Claude.

6. References

Audry, S., Schäfer, J., Blanc, G., & Jouanneau, J. M. (2004). Fifty-year sedimentary record of heavy metal pollution (Cd, Zn, Cu, Pb) in the Lot River reservoirs (France). *Environmental Pollution*, *132*(3), 413-426.

Arnaud, F., Schmitt, L., Johnstone, K., Rollet, A. J., & Piégay, H. (2019). Engineering impacts on the Upper Rhine channel and floodplain over two centuries. *Geomorphology*, *330*, 13-27.

Arnaud-Fassetta, G. (2003). River channel changes in the Rhone Delta (France) since the end of the Little Ice Age: geomorphological adjustment to hydroclimatic change and natural resource management. *Catena*, *51*(2), 141-172.

Attal, M. (2017). Linkage between sediment transport and supply in mountain rivers. Gravel-Bed Rivers, 329-353.

Bábek, O., Faměra, M., Hilscherová, K., Kalvoda, J., Dobrovolný, P., Sedláček, J., ... & Holoubek, I. (2011). Geochemical traces of flood layers in the fluvial sedimentary archive; implications for contamination history analyses. *Catena*, *87*(2), 281-290.

Bábek, O., Hilscherová, K., Nehyba, S., Zeman, J., Famera, M., Francu, J., ... & Klánová, J. (2008). Contamination history of suspended river sediments accumulated in oxbow lakes over the last 25 years. *Journal of Soils and Sediments*, *8*(3), 165-176.

Bábek, O., Kielar, O., Lenďáková, Z., Mandlíková, K., Sedláček, J., & Tolaszová, J. (2020). Reservoir deltas and their role in pollutant distribution in valley-type dam reservoirs: Les Království Dam, Elbe River, Czech Republic. *Catena*, *184*, 104251.

Belletti, B., de Leaniz, C. G., Jones, J., Bizzi, S., Börger, L., Segura, G., ... & Zalewski, M. (2020). More than one million barriers fragment Europe's rivers. *Nature*, *588*(7838), 436-441.

Bergé, A., Cladière, M., Gasperi, J., Coursimault, A., Tassin, B., & Moilleron, R. (2013). Meta-analysis of environmental contamination by phthalates. *Environmental Science and Pollution Research*, *20*(11), 8057-8076.

Best, J. (2019). Anthropogenic stresses on the world's big rivers. *Nature Geoscience*, *12*(1), 7-21.

Borselli, L., Cassi, P., & Torri, D. (2008). Prolegomena to sediment and flow connectivity in the landscape: a GIS and field numerical assessment. *Catena*, *75*(3), 268-277.

Bossy, A., Grosbois, C., Beauchemin, S., Courtin-Nomade, A., Hendershot, W., & Bril, H. (2010). Alteration of As-bearing phases in a small watershed located on a high grade arsenic-geochemical anomaly (French Massif Central). *Applied Geochemistry*, *25*(12), 1889-1901.

Bravard, J. P. (1999). Le flottage du bois et le changement du paysage fluvial des montagnes françaises. *Médiévales*, 53-61.

Bravard J.-P., Landon N., Franceschi C., (1998). Etude geomorphologique de la basse Bienne entre les retenues d'Etables et de Coiselet

Brenna, A., Surian, N., & Mao, L. (2020). Response of A Gravel-Bed River To Dam Closure: Insights From Sediment Transport Processes And Channel Morphodynamics. *Earth Surface Processes and Landforms*, *45*(3), 756-770.

Breivik, K., Sweetman, A., Pacyna, J. M., and Jones, K. C.: (2002a) Towards a global historical emission inventory for selected PCB congeners — a mass balance approach. 1. Global production and consumption, Sci. Total Environ., 290, 181–198.

Breivik, K., Sweetman, A., Pacyna, J. M., and Jones, K. C.:(2002b) Towards a global historical emission inventory for selected PCB congeners – a mass balance approach: 2. Emissions, Sci. Total Environ., 290, 199–224.

Breivik, K., Sweetman, A., Pacyna, J. M., and Jones, K. C.: (2007) Towards a global historical emission inventory for selected PCB congeners – a mass balance approach. 3. An update, Sci. Total Environ., 377, 296–307.

Brils, J. (2020). Including sediment in European River Basin Management Plans: twenty years of work by SedNet. Journal of Soils and Sediments, 20(12), 4229-4237.

Burt, T. P., & Allison, R. J. (2010). Sediment cascades in the environment: An integrated approach. *Sediment cascades: An integrated approach*, 1-16.

Bussi, G., Darby, S. E., Whitehead, P. G., Jin, L., Dadson, S. J., Voepel, H. E., ... & Nicholas, A. (2021). Impact of dams and climate change on suspended sediment flux to the Mekong delta. *Science of the Total Environment*, *755*, 142468.

Casserly, C. M., Turner, J. N., O'Sullivan, J. J., Bruen, M., Bullock, C., Atkinson, S., & Kelly-Quinn, M. (2020). Impact of low-head dams on bedload transport rates in coarse-bedded streams. *Science of The Total Environment*, *716*, 136908.

Casserly, C. M., Turner, J. N., O'Sullivan, J. J., Bruen, M., Bullock, C., Atkinson, S., & Kelly-Quinn, M. (2021). Effect of low-head dams on reach-scale suspended sediment dynamics in coarse-bedded streams. *Journal of Environmental Management*, *277*, 111452.

Chabert, L. (1978). Vallées montagnardes et industrie: le cas des Alpes françaises du nord (Mountain valleys and industry: the example of the northern french Alps). *Bulletin de l'Association de Géographes Français*, *55*(453), 187-191.

Charles, M. J., & Hites, R. A. (1987). Sediments as archives of environmental pollution trends.

Colas, F., BAUDOIN, J. M., Danger, M., Usseglio-Polatera, P. H. I. L. I. P. P. E., Wagner, P., & Devin, S. (2013). Synergistic impacts of sediment contamination and dam presence on river functioning. *Freshwater Biology*, *58*(2), 320-336.

Church, M., & Zimmermann, A. (2007). Form and stability of step-pool channels: Research progress. Water Resources Research, 43(3).

Courtin-Nomade, A., Waltzing, T., Evrard, C., Soubrand, M., Lenain, J.F., Ducloux, E., Ghorbel, S., Grosbois, C., Bril, H. 2016. Arsenic and lead mobility: from tailing materials to the aqueous compartment. App. Geochem., 64, 10-21.

Coynel, A., Schäfer, J., Blanc, G., & Bossy, C. (2007). Scenario of particulate trace metal and metalloid transport during a major flood event inferred from transient geochemical signals. *Applied Geochemistry*, *22*(4), 821-836.

Dade, W. B., & Friend, P. F. (1998). Grain-size, sediment-transport regime, and channel slope in alluvial rivers. The Journal of Geology, 106(6), 661-676.

de Deckere, E., De Cooman, W., Leloup, V., Meire, P., Schmitt, C., & Peter, C. (2011). Development of sediment quality guidelines for freshwater ecosystems. *Journal of soils and sediments*, *11*(3), 504-517.

Dendievel, A. M., Grosbois, C., Ayrault, S., Evrard, O., Coynel, A., Debret, M., ... & Mourier, B. (2022). Key factors influencing metal concentrations in sediments along Western European Rivers: A long-term monitoring study (1945–2020). Science of the Total Environment, 805, 149778.

Dendievel, A. M., Mourier, B., Coynel, A., Evrard, O., Labadie, P., Ayrault, S., ... & Desmet, M. (2020a). Spatio-temporal assessment of the polychlorinated biphenyl (PCB) sediment contamination in four major French river corridors (1945–2018). *Earth System Science Data*, *12*(2), 1153-1170.

Dendievel, A. M., Mourier, B., Dabrin, A., Delile, H., Coynel, A., Gosset, A., ... & Bedell, J. P. (2020b). Metal pollution trajectories and mixture risk assessed by combining dated cores and subsurface sediments along a major European river (Rhône River, France). *Environment International*, *144*, 106032.

Desmet, M., Mourier, B., Mahler, B. J., Van Metre, P. C., Roux, G., Persat, H., ... & Babut, M. (2012). Spatial and temporal trends in PCBs in sediment along the lower Rhône River, France. Science of the Total Environment, 433, 189-197.

Directive 2008105EC of the European Parliament and the Council of 16 December 2008 of Environmental Quality Standards in the Field of Water Policy, Amending and Subsequently Repealing Council Directives 82176 EEC, 83513 EEC, 84156 EEC, 86280 EEC and Amending DDhivert, E., Grosbois, C., Courtin-Nomade, A., Bourrain, X., & Desmet, M. (2016). Dynamics of metallic contaminants at a basin scale—spatial and temporal reconstruction from four sediment cores (Loire fluvial system, France). *Science of the total environment*, *541*, 1504-1515.

Dhivert, E., Grosbois, C., Coynel, A., Lefèvre, I., & Desmet, M. (2015a). Influences of major flood sediment inputs on sedimentary and geochemical signals archived in a reservoir core (Upper Loire Basin, France). *Catena*, *126*, 75-85.

Dhivert, E., Grosbois, C., Rodrigues, S., & Desmet, M. (2015b). Influence of fluvial environments on sediment archiving processes and temporal pollutant dynamics (Upper Loire River, France). *Science of the total Environment*, *505*, 121-136.

Dong, M., Chen, W., Chen, X., Xing, X., Shao, M., Xiong, X., & Luo, Z. (2021). Geochemical markers of the Anthropocene: Perspectives from temporal trends in pollutants. Science of The Total Environment, 763, 142987.

Donovan, M., Miller, A., Baker, M., & Gellis, A. (2015). Sediment contributions from floodplains and legacy sediments to Piedmont streams of Baltimore County, Maryland. *Geomorphology*, *235*, 88-105.

Downs, P. W., & Piégay, H. (2019). Catchment-scale cumulative impact of human activities on river channels in the late Anthropocene: implications, limitations, prospect. *Geomorphology*, *338*, 88-104.

Dufour, S., & Piégay, H. (2010). Channel vertical mobility, hydro-geomorphic disturbances and understory vegetation in floodplain forests of the Ain River (France). *Géomorphologie: relief, processus, environnement*, *16*(4), 371-386.

Ettler, V., Mihaljevič, M., Šebek, O., Molek, M., Grygar, T., & Zeman, J. (2006). Geochemical and Pb isotopic evidence for sources and dispersal of metal contamination in stream sediments from the mining and smelting district of Příbram, Czech Republic. *Environmental pollution*, *142*(3), 409-417.

Ettler, V., Vaněk, A., Mihaljevič, M., & Bezdička, P. (2005). Contrasting lead speciation in forest and tilled soils heavily polluted by lead metallurgy. *Chemosphere*, *58*(10), 1449-1459.

Fazelpoor, K., Martínez-Fernández, V., & de Jalón, D. G. (2021). Exploring the hydromorphological response to human pressure in Tagus River (1946–2014) by complementary diagnosis. *CATENA*, *198*, 105052.

Ferrand, E., Eyrolle, F., Radakovitch, O., Provansal, M., Dufour, S., Vella, C., ... & Gurriaran, R. (2012). Historical levels of heavy metals and artificial radionuclides reconstructed from overbank sediment records in lower Rhône River (South-East France). *Geochimica et Cosmochimica Acta*, *82*, 163-182.

Fencl, J. S., Mather, M. E., Costigan, K. H., & Daniels, M. D. (2015). How big of an effect do small dams have? Using geomorphological footprints to quantify spatial impact of low-head dams and identify patterns of across-dam variation. PLoS one, 10(11), e0141210.

Fleming, P. M., Merritts, D. J., & Walter, R. C. (2019). Legacy sediment erosion hot spots: A cost-effective approach for targeting water quality improvements. *Journal of Soil and Water Conservation*, *74*(4), 67A-73A.

Folk, R. L., & Ward, W. C. (1957). Brazos River bar [Texas]; a study in the significance of grain size parameters. *Journal of Sedimentary Research*, *27*(1), 3-26.

Förstner, U. (2004). Sediment dynamics and pollutant mobility in rivers: an interdisciplinary approach. *Lakes & Reservoirs: Research & Management*, *9*(1), 25-40.

Foucher, A., Chaboche, P. A., Sabatier, P., & Evrard, O. (2021). A worldwide meta-analysis (1977–2020) of sediment core dating using fallout radionuclides including 137 Cs and 210 Pb xs. Earth System Science Data, 13(10), 4951-4966.

Frémion, F., Bordas, F., Mourier, B., Lenain, J. F., Kestens, T., & Courtin-Nomade, A. (2016). Influence of dams on sediment continuity: a study case of a natural metallic contamination. *Science of the Total Environment*, *547*, 282-294.

Fryirs, K. (2013). (Dis) Connectivity in catchment sediment cascades: a fresh look at the sediment delivery problem. Earth Surface Processes and Landforms, 38(1), 30-46.

Fryirs, K. A. (2017). River sensitivity: A lost foundation concept in fluvial geomorphology. Earth Surface Processes and Landforms, 42(1), 55-70.

Gałuszka, A., Migaszewski, Z. M., & Zalasiewicz, J. (2014). Assessing the Anthropocene with geochemical methods. *Geological Society, London, Special Publications*, *395*(1), 221-238.

Gao, D. W., & Wen, Z. D. (2016). Phthalate esters in the environment: A critical review of their occurrence, biodegradation, and removal during wastewater treatment processes. *Science of the total Environment*, *541*, 986-1001.

Gardes, T., Debret, M., Copard, Y., Patault, E., Winiarski, T., Develle, A. L., ... & Portet-Koltalo, F. (2020). Reconstruction of anthropogenic activities in legacy sediments from the Eure River, a major tributary of the Seine Estuary (France). *Catena*, *190*, 104513.

Gardes, T., Portet-Koltalo, F., Debret, M., Humbert, K., Levaillant, R., Simon, M., & Copard, Y. (2020). Temporal trends, sources, and relationships between sediment characteristics and polycyclic aromatic hydrocarbons (PAHs) and polychlorinated biphenyls (PCBs) in sediment cores from the major Seine estuary tributary, France. *Applied Geochemistry*, *122*, 104749.

Gasowski, Z. (1994). L'enfoncement du lit de la Loire/the entrenchment of the Loire's river bed. *Géocarrefour*, *69*(1), 41-45.

Gaspar, L., Lizaga, I., Latorre, B., Blake, W. H., & Navas, A. (2018, April). Testing FingerPro mixing model using experimental sediment mixtures. In *EGU General Assembly Conference Abstracts* (p. 14068).

Gałuszka, A., Migaszewski, Z. M., & Rose, N. L. (2020). A consideration of polychlorinated biphenyls as a chemostratigraphic marker of the Anthropocene. The Anthropocene Review, 7(2), 138-158.

Graham, P. R. (1973). Phthalate ester plasticizers–why and how they are used. Environ. Health Perspect. 3, 3–12.

Grill, G., Lehner, B., Lumsdon, A. E., MacDonald, G. K., Zarfl, C., & Liermann, C. R. (2015). An index-based framework for assessing patterns and trends in river fragmentation and flow regulation by global dams at multiple scales. *Environmental Research Letters*, *10*(1), 015001.

Grill, G., Lehner, B., Thieme, M., Geenen, B., Tickner, D., Antonelli, F., ... & Zarfl, C. (2019). Mapping the world's free-flowing rivers. *Nature*, *569*(7755), 215-221.

Grosbois, C., & Courtin-Nomade, A. (2019). Microscale distribution of trace elements: a methodology for accessing major bearing phases in stream sediments as applied to the Loire basin (France). *Journal of Soils and Sediments*, *20*(1), 498-512.

Grosbois, C., Meybeck, M., Lestel, L., Lefèvre, I., & Moatar, F. (2012). Severe and contrasted polymetallic contamination patterns (1900–2009) in the Loire River sediments (France). *Science of the total environment*, *435*, 290-305.

Grousset, F. E., Jouanneau, J. M., Castaing, P., Lavaux, G., & Latouche, C. (1999). A 70 year record of contamination from industrial activity along the Garonne River and its tributaries (SW France). *Estuarine, Coastal and Shelf Science*, *48*(3), 401-414.

Grygar, T. M., Elznicová, J., Kiss, T., & Smith, H. G. (2016). Using sedimentary archives to reconstruct pollution history and sediment provenance: The Ohře River, Czech Republic. *Catena*, *144*, 109-129.

Grygar, T. M., Hošek, M., Pacina, J., Štojdl, J., Bábek, O., Sedláček, J., ... & Tolaszová, J. (2018). Changes in the geochemistry of fluvial sediments after dam construction (the Chrudimka River, the Czech Republic). *Applied Geochemistry*, *98*, 94-108.

Grygar, T. M., Sedláček, J., Bábek, O., Nováková, T., Strnad, L., & Mihaljevič, M. (2012). Regional contamination of Moravia (South-Eastern Czech Republic): temporal shift of Pb and Zn loading in fluvial sediments. *Water, Air, & Soil Pollution*, *223*(2), 739-753.

Habersack, H., Hein, T., Stanica, A., Liska, I., Mair, R., Jäger, E., ... & Bradley, C. (2016). Challenges of river basin management: current status of, and prospects for, the River Danube from a river engineering perspective. *Science of the Total Environment*, *543*, 828-845.

Heim, S., & Schwarzbauer, J. (2013). Pollution history revealed by sedimentary records: a review. *Environmental chemistry letters*, *11*(3), 255-270.

Horacio, J., Ollero, A., Noguera, I., & Fernández-Pasquier, V. (2019). Flooding, channel dynamics and transverse infrastructure: a challenge for Middle Ebro river management. *Journal of Maps*, *15*(2), 310-319.

Horowitz, A. J., & Elrick, K. A. (1987). The relation of stream sediment surface area, grain size and composition to trace element chemistry. *Applied geochemistry*, *2*(4), 437-451.

Jamarani, R., Erythropel, H. C., Nicell, J. A., Leask, R. L., & Marić, M. (2018). How green is your plasticizer?. *Polymers*, *10*(8), 834.James, L. A. (2017). Arrested geomorphic trajectories and the long-term hidden potential for change. *Journal of environmental management*, *202*, 412-423.

Janod, R. (1985). Les radeliers de la vallée de la Bienne (Jura). *Le Monde alpin et rhodanien. Revue régionale d'ethnologie*, *13*(4), 41-54.

Jasminka, A., & Robert, Š. (2011). Distribution of chemical elements in an old metallurgical area, Zenica (Bosnia and Herzegovina). *Geoderma*, *162*(1-2), 71-85.

Jiang, G., Lutgen, A., Mattern, K., Sienkiewicz, N., Kan, J., & Inamdar, S. (2020). Streambank Legacy Sediment Contributions to Suspended Sediment-Bound Nutrient Yields from a Mid-Atlantic, Piedmont Watershed. JAWRA Journal of the American Water Resources Association, 56(5), 820-841.

Jourdain, C., Claude, N., Tassi, P., Cordier, F., & Antoine, G. (2020). Morphodynamics of alternate bars in the presence of riparian vegetation. *Earth Surface Processes and Landforms*, *45*(5), 1100-1122.

Jumani, S., Deitch, M. J., Kaplan, D., Anderson, E. P., Krishnaswamy, J., Lecours, V., & Whiles, M. R. (2020). River fragmentation and flow alteration metrics: a review of methods and directions for future research. *Environmental Research Letters*.

Kaushal, S. S., Gold, A. J., Bernal, S., Johnson, T. A. N., Addy, K., Burgin, A., ... & Belt, K. T. (2018). Watershed 'chemical cocktails': forming novel elemental combinations in Anthropocene fresh waters. *Biogeochemistry*, *141*(3), 281-305.

Kim, S., Kim, Y., & Moon, H. B. (2021). Contamination and historical trends of legacy and emerging plasticizers in sediment from highly industrialized bays of Korea. Science of The Total Environment, 765, 142751.Kleinhans, M. G., & van den Berg, J. H. (2011). River channel and bar patterns explained and predicted by an empirical and a physics-based method. Earth Surface Processes and Landforms, 36(6), 721-738.

Kus, A., Unver, E., Jagger, B., & Durgun, I. (2013). A study of injection moulding with bismuth alloy. *Green Design, Materials and Manufacturing Processes*, 225-232.

Lane, E. W. (1955). The importance of fluvial morphology in hydraulic engineering: Proceedings–American Society of Civil Engineers, v. 81.

Lane, S. N., Tayefi, V., Reid, S. C., Yu, D., & Hardy, R. J. (2007). Interactions between sediment delivery, channel change, climate change and flood risk in a temperate upland environment. *Earth*

Surface Processes and Landforms: The Journal of the British Geomorphological Research Group, *32*(3), 429-446.

Landon N., Bravard J.-P., Franceschi C., 1998 : Etude du fonctionnement physique de la basse vallée de la Bienne (Jura). Rapport d'expertise pour le compte du P.N.R. du Haut-Jura, 99 p

Landon N., Bravard J.-P., Leméhauté N., 2000 : Etude des processus de recharge sédimentaire du bassin versant de la Bienne (Jura), du transit de la charge de fond et de l'impact des aménagements sur celui-ci. Rapport d'expertise pour le compte du P.N.R. du Haut-Jura, 183 p

Latapie, A., Camenen, B., Rodrigues, S., Paquier, A., Bouchard, J. P., & Moatar, F. (2014). Assessing channel response of a long river influenced by human disturbance. *Catena*, *121*, 1-12.

Lecce, S. A., & Pavlowsky, R. T. (2014). Floodplain storage of sediment contaminated by mercury and copper from historic gold mining at Gold Hill, North Carolina, USA. Geomorphology, 206, 122-132.

Le Cloarec, M. F., Bonte, P. H., Lestel, L., Lefèvre, I., & Ayrault, S. (2011). Sedimentary record of metal contamination in the Seine River during the last century. *Physics and Chemistry of the Earth, Parts A/B/C*, *36*(12), 515-529.

Ledieu, L., Simonneau, A., Cerdan, O., Négrel, P., Laperche, V., Grosbois, C., & Laggoun-Défarge, F. (2020). Geochemical insights into spatial and temporal evolution of sediment at catchment scale (Egoutier stream, France). *Applied Geochemistry*, *122*, 104743.

Lenzi, M. A., Mao, L., & Comiti, F. (2006). Effective discharge for sediment transport in a mountain river: Computational approaches and geomorphic effectiveness. Journal of Hydrology, 326(1-4), 257-276.

Li, X., Han, X., Vogt, R. D., Zhou, J., Zheng, B., Song, Y., & Lu, X. (2021). Distributions, temporal trends and ecological risks of polyethylene terephthalate (PET) and di-(2-ethylhexyl) phthalate (DEHP) in sediments of Jiaozhou Bay, China. Marine Pollution Bulletin, 165, 112176.Lizaga, I., Latorre, B., Gaspar, L., & Navas, A. (2018, April). FingerPro mixing model: An R package for sediment tracing. In *EGU General Assembly Conference Abstracts* (p. 3752).

Lizaga, I., Latorre, B., Gaspar, L., & Navas, A. (2020). FingerPro: an R Package for Tracking the Provenance of Sediment. *Water Resources Management*, *34*(12), 3879-3894.

Lorgeoux, C., Moilleron, R., Gasperi, J., Ayrault, S., Bonté, P., Lefèvre, I., & Tassin, B. (2016). Temporal trends of persistent organic pollutants in dated sediment cores: chemical fingerprinting of the anthropogenic impacts in the Seine River basin, Paris. *Science of the Total Environment*, *541*, 1355-1363.

Lyons, N. J., Starek, M. J., Wegmann, K. W., & Mitasova, H. (2015). Bank erosion of legacy sediment at the transition from vertical to lateral stream incision. *Earth Surface Processes and Landforms*, *40*(13), 1764-1778.

Marren, P. M., Grove, J. R., Webb, J. A., & Stewardson, M. J. (2014). The potential for dams to impact lowland meandering river floodplain geomorphology. The Scientific World Journal, 2014.

Marston, R. A., Girel, J., Pautou, G., Piégay, H., Bravard, J. P., & Arneson, C. (1995). Channel metamorphosis, floodplain disturbance, and vegetation development: Ain River, France. *Geomorphology*, *13*(1-4), 121-131.

McMahon, P., Beauchamp, V. B., Casey, R. E., Salice, C. J., Bucher, K., Marsh, M., & Moore, J. (2021). Effects of stream restoration by legacy sediment removal and floodplain reconnection on water quality. *Environmental Research Letters*, *16*(3), 035009.

Meusburger, K., Evrard, O., Alewell, C., Borrelli, P., Cinelli, G., Ketterer, M., ... & Ballabio, C. (2020). Plutonium aided reconstruction of caesium atmospheric fallout in European topsoils. *Scientific reports*, *10*(1), 1-16.

Meybeck, M. (2002). Riverine quality at the Anthropocene: Propositions for global space and time analysis, illustrated by the Seine River. *Aquatic Sciences*, *64*(4), 376-393.

Meybeck, M. (2003). Global analysis of river systems: from Earth system controls to Anthropocene syndromes. *Philosophical Transactions of the Royal Society of London. Series B: Biological Sciences*, *358*(1440), 1935-1955.

Meybeck, M., Horowitz, A. J., & Grosbois, C. (2004). The geochemistry of Seine River Basin particulate matter: distribution of an integrated metal pollution index. *Science of the total environment*, *328*(1-3), 219-236.

Meybeck, M., Lestel, L., Carré, C., Bouleau, G., Garnier, J., & Mouchel, J. M. (2018). Trajectories of river chemical quality issues over the Longue Durée: the Seine River (1900S–2010). *Environmental Science and Pollution Research*, *25*(24), 23468-23484.

Middelkoop, H. (2000). Heavy-metal pollution of the river Rhine and Meuse floodplains in the Netherlands. *Netherlands journal of geosciences*, *79*(4), 411-427.

Mourier, B., Desmet, M., Van Metre, P. C., Mahler, B. J., Perrodin, Y., Roux, G., ... & Babut, M. (2014). Historical records, sources, and spatial trends of PCBs along the Rhône River (France). *Science of the total environment*, *476*, 568-576.

Mourier, B., Labadie, P., Desmet, M., Grosbois, C., Raux, J., Debret, M., ... & Babut, M. (2019). Combined spatial and retrospective analysis of fluoroalkyl chemicals in fluvial sediments reveal changes in levels and patterns over the last 40 years. *Environmental Pollution*, *253*, 1117-1125.

Mueller, E. R., & Pitlick, J. (2013). Sediment supply and channel morphology in mountain river systems: 2. Single thread to braided transitions. Journal of Geophysical Research: Earth Surface, 119(7), 1516-1541.

Mulder, K., & Knot, M. (2001). PVC plastic: a history of systems development and entrenchment. *Technology in Society*, *23*(2), 265-286.

Nagorka, R., & Koschorreck, J. (2020). Trends for plasticizers in German freshwater environments–Evidence for the substitution of DEHP with emerging phthalate and non-phthalate alternatives. *Environmental Pollution*, *262*, 114237.

Najafi, S., Dragovich, D., Heckmann, T., & Sadeghi, S. H. (2021). Sediment connectivity concepts and approaches. *Catena*, *196*, 104880.

Net, S., Sempere, R., Delmont, A., Paluselli, A., & Ouddane, B. (2015). Occurrence, fate, behavior and ecotoxicological state of phthalates in different environmental matrices. Environmental Science & Technology, 49(7), 4019-4035.

Noe, G. B., Cashman, M. J., Skalak, K., Gellis, A., Hopkins, K. G., Moyer, D., ... & Hupp, C. (2020). Sediment dynamics and implications for management: State of the science from long-term research in the Chesapeake Bay watershed, USA. *Wiley Interdisciplinary Reviews: Water*, *7*(4), e1454.

O'Brien, G. R., Wheaton, J., Fryirs, K., McHugh, P., Bouwes, N., Brierley, G., & Jordan, C. (2017). A geomorphic assessment to inform strategic stream restoration planning in the Middle Fork John Day Watershed, Oregon, USA. Journal of Maps, 13(2), 369-381.

Ojebuoboh, F. K. (1992). Bismuth—Production, properties, and applications. *JOM*, *44*(4), 46-49.

Ogilvie, S. C. (1993). Proto-industrialization in Europe. *Continuity and Change*, *8*(2), 159-179.

Paravy, A., Tournery, J.-F. (1973): Aménagement de l'Ain: le barrage de Coiselet. Dans: Travaux, n. 458 (mai 1973), pp. 11.

Parrinello, G. (2018). Systems of power: a spatial envirotechnical approach to water power and industrialization in the po valley of Italy, ca. 1880–1970. *Technology and culture*, *59*(3), 652-688.

Pavlowsky, R. T., Lecce, S. A., Owen, M. R., & Martin, D. J. (2017). Legacy sediment, lead, and zinc storage in channel and floodplain deposits of the Big River, Old Lead Belt Mining District, Missouri, USA. Geomorphology, 299, 54-75.

Peterson, J. C., & Freeman, D. H. (1982). Phthalate ester concentration variations in dated sediment cores from the Chesapeake Bay [USA]. Environmental Science & Technology, 16(8), 464-469.

Petit, F., Poinsart, D., & Bravard, J. P. (1996). Channel incision, gravel mining and bedload transport in the Rhône river upstream of Lyon, France ("canal de Miribel"). *Catena*, *26*(3-4), 209-226.

Pitlick, J., Mueller, E. R., Segura, C., Cress, R., & Torizzo, M. (2008). Relation between flow, surface-layer armoring and sediment transport in gravel-bed rivers. *Earth Surface Processes and Landforms: The Journal of the British Geomorphological Research Group*, *33*(8), 1192-1209.

Pizzuto, J. E. (2014). Long-term storage and transport length scale of fine sediment: Analysis of a mercury release into a river. Geophysical Research Letters, 41(16), 5875-5882.

Piégay, H. (2016). System approaches in fluvial geomorphology. In Kondolf, M., Piégay, H. Tools in Fluvial Geomorphology, 5, 75–102

Piégay, H., Arnaud, F., Belletti, B., Bertrand, M., Bizzi, S., Carbonneau, P., ... & Slater, L. (2020). Remotely sensed rivers in the Anthropocene: State of the art and prospects. *Earth Surface Processes and Landforms*, *45*(1), 157-188.

Piégay, H., Hupp, C. R., Citterio, A., Dufour, S., Moulin, B., & Walling, D. E. (2008). Spatial and temporal variability in sedimentation rates associated with cutoff channel infill deposits: Ain River, France. *Water Resources Research*, *44*(5).

Pirkhoffer, E., Halmai, Á., Ficsor, J., Gradwohl-Valkay, A., Lóczy, D., Nagy, Á., ... & Czigány, S. (2021). Bedload entrainment dynamics in a partially channelized river with mixed bedload: A case study of the Drava River, Hungary. River Research and Applications.

Provansal, M., Dufour, S., Sabatier, F., Anthony, E. J., Raccasi, G., & Robresco, S. (2014). The geomorphic evolution and sediment balance of the lower Rhône River (southern France) over the last 130 years: Hydropower dams versus other control factors. *Geomorphology*, *219*, 27-41.

Recking, A. (2012). Influence of sediment supply on mountain streams bedload transport. Geomorphology, 175, 139-150.

Reis, A., Parker, A., & Alencoão, A. (2014). Storage and origin of metals in active stream sediments from mountainous rivers: a case study in the River Douro basin (North Portugal). *Applied geochemistry*, *44*, 69-79.

Resongles, E., Casiot, C., Freydier, R., Dezileau, L., Viers, J., & Elbaz-Poulichet, F. (2014). Persisting impact of historical mining activity to metal (Pb, Zn, Cd, Tl, Hg) and metalloid (As, Sb) enrichment in sediments of the Gardon River, Southern France. Science of the Total Environment, 481, 509-521.

Rodrigues, S., Bréhéret, J. G., Macaire, J. J., Greulich, S., & Villar, M. (2007). In-channel woody vegetation controls on sedimentary processes and the sedimentary record within alluvial environments: a modern example of an anabranch of the River Loire, France. *Sedimentology*, *54*(1), 223-242.

Schumm, S. A. (1985). Patterns of alluvial rivers. Annual Review of Earth and Planetary Sciences, 13(1), 5-27.

Szalińska, E., Orlińska-Woźniak, P., & Wilk, P. (2020). Sediment load variability in response to climate and land use changes in a Carpathian catchment (Raba River, Poland). *Journal of Soils and Sediments*, 1-12.

Sokolov, D. I., Erina, O. N., Tereshina, M. A., & Puklakov, V. V. (2020). Impact Of Mozhaysk Dam On The Moscow River Sediment Transport. *GEOGRAPHY, ENVIRONMENT, SUSTAINABILITY*, *13*(4), 24-31.

Steffen, W., Sanderson, R. A., Tyson, P. D., Jäger, J., Matson, P. A., Moore III, B., ... & Wasson, R. J. (2004). *Global change and the earth system: a planet under pressure*. Springer Science & Business Media.

Steffen W, Crutzen PJ, McNeill JR. 2007. The Anthropocene: are humans now overwhelming the great forces of nature? Ambio 16 (8): 614–621.

Steffen, W., Broadgate, W., Deutsch, L., Gaffney, O., & Ludwig, C. (2015). The trajectory of the Anthropocene: the great acceleration. *The Anthropocene Review*, *2*(1), 81-98.

Surian, N., & Rinaldi, M. (2003). Morphological response to river engineering and management in alluvial channels in Italy. *Geomorphology*, *50*(4), 307-326.

Thiebault, T., Alliot, F., Berthe, T., Blanchoud, H., Petit, F., & Guigon, E. (2021). Record of trace organic contaminants in a river sediment core: from historical wastewater management to historical use. *Science of the Total Environment*, 145694.

Tockner, K., Uehlinger, U., & Robinson, C. T. (2009). *Rivers of Europe*. Academic Press.

Vauclin, S., Mourier, B., Dendievel, A. M., Marchand, P., Vénisseau, A., Morereau, A., ... & Winiarski, T. (2021). Temporal trends of legacy and novel brominated flame retardants in sediments along the Rhône River corridor in France. *Chemosphere*, 129889.

Vauclin, S., Mourier, B., Dendievel, A. M., Noclin, N., Piégay, H., Marchand, P., ... & Winiarski, T. (2020a). Depositional environments and historical contamination as a framework to reconstruct fluvial sedimentary evolution. *Science of the Total Environment*, 142900.

Vauclin, S., Mourier, B., Piégay, H., & Winiarski, T. (2020b). Legacy sediments in a European context: The example of infrastructure-induced sediments on the Rhône River. *Anthropocene*, *31*, 100248.

Vauclin, S., Mourier, B., Tena, A., Piégay, H., & Winiarski, T. (2019). Effects of river infrastructures on the floodplain sedimentary environment in the Rhône River. *Journal of Soils and Sediments*, 1-12.

Versaci, R., Minniti, F., Foti, G., Canale, C., & Barillà, G. C. (2018). River anthropization: Case studies in Reggio Calabria, Italy. *WIT Transactions on Ecology and the Environment*, *217*, 903-912.

Vörösmarty, C. J., Meybeck, M., Fekete, B., Sharma, K., Green, P., & Syvitski, J. P. (2003). Anthropogenic sediment retention: major global impact from registered river impoundments. *Global and planetary change*, *39*(1-2), 169-190.

Vukovic, D., Vukovic, Z., & Stankovic, S. (2014). The impact of the Danube Iron Gate Dam on heavy metal storage and sediment flux within the reservoir. *Catena*, *113*, 18-23.

Walling, D. E. (2009). The sediment load of the Mekong River. In *The Mekong* (pp. 113-142). Academic Press.

Walling, D. E., Owens, P. N., Carter, J., Leeks, G. J. L., Lewis, S., Meharg, A. A., & Wright, J. (2003). Storage of sediment-associated nutrients and contaminants in river channel and floodplain systems. *Applied geochemistry*, *18*(2), 195-220.

Wintenberger, C. L., Rodrigues, S., Bréhéret, J. G., & Villar, M. (2015). Fluvial islands: First stage of development from nonmigrating (forced) bars and woody-vegetation interactions. *Geomorphology*, *246*, 305-320.

Yager, E. M., Turowski, J. M., Rickenmann, D., & McArdell, B. W. (2012). Sediment supply, grain protrusion, and bedload transport in mountain streams. Geophysical Research Letters, 39(10).

Zhu, H., Bing, H., Wu, Y., Zhou, J., Sun, H., Wang, J., & Wang, X. (2019). The spatial and vertical distribution of heavy metal contamination in sediments of the Three Gorges Reservoir determined by anti-seasonal flow regulation. *Science of the Total Environment*, *664*, 79-88.

Figures and tables

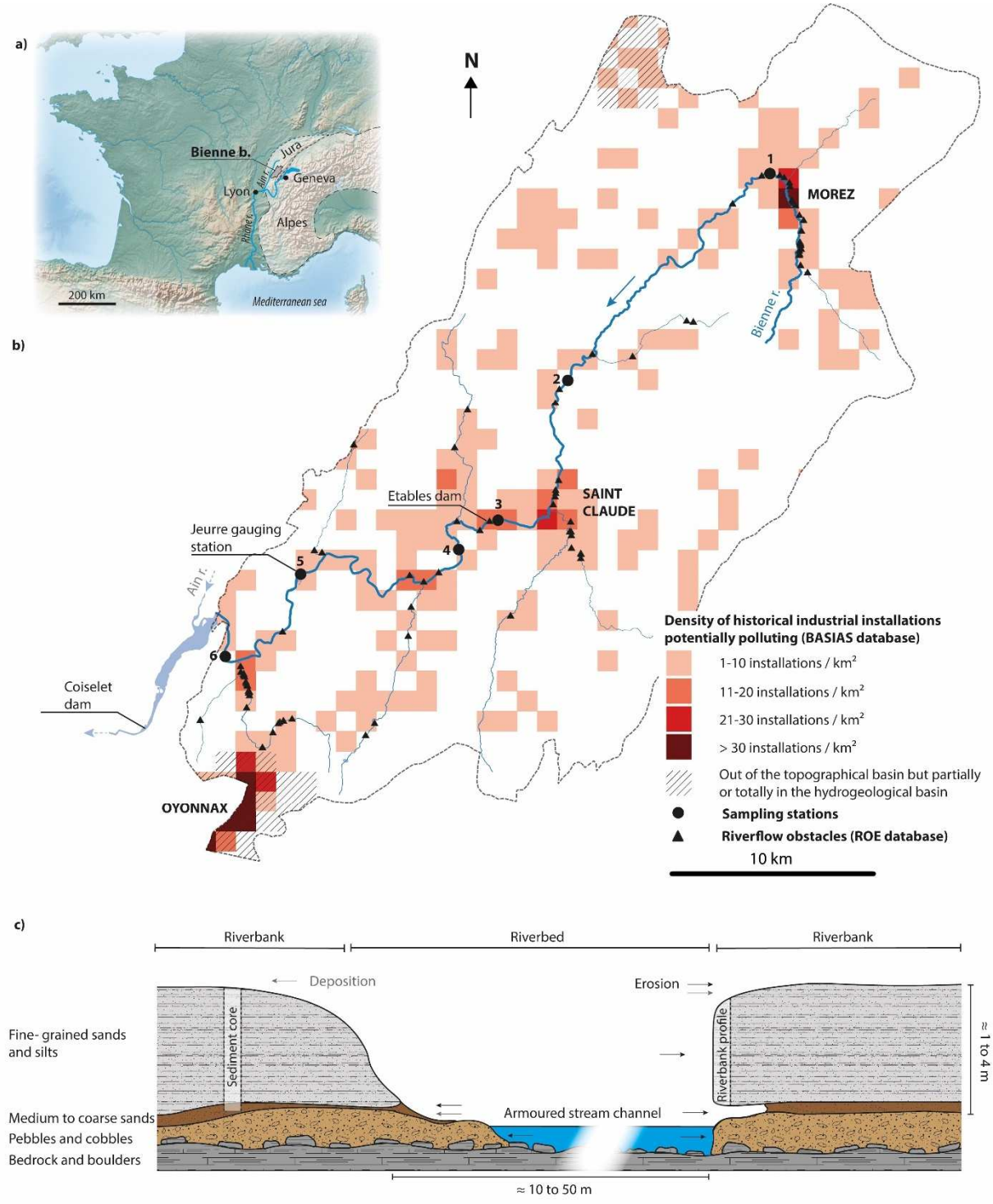

Figure 1. a) Location of the Bienne basin (Bienne b.) in Western Europe (Copernicus database, www.copernicus.eu). b) Hydrography, catchment limit (Carthage and BDLISA databases,www.data.gouv.fr), density of historical and current industrial installations calculated at 1 km² pixel size (Basias database, www.georisques.gouv.fr), referenced river flow obstacles (dams and sills; ROE database, www.data.gouv.fr), and positions of sampling stations along the Bienne basin. c) Schematic view of the Bienne riverbanks and sampling plan (sedimentary core and riverbank profile).

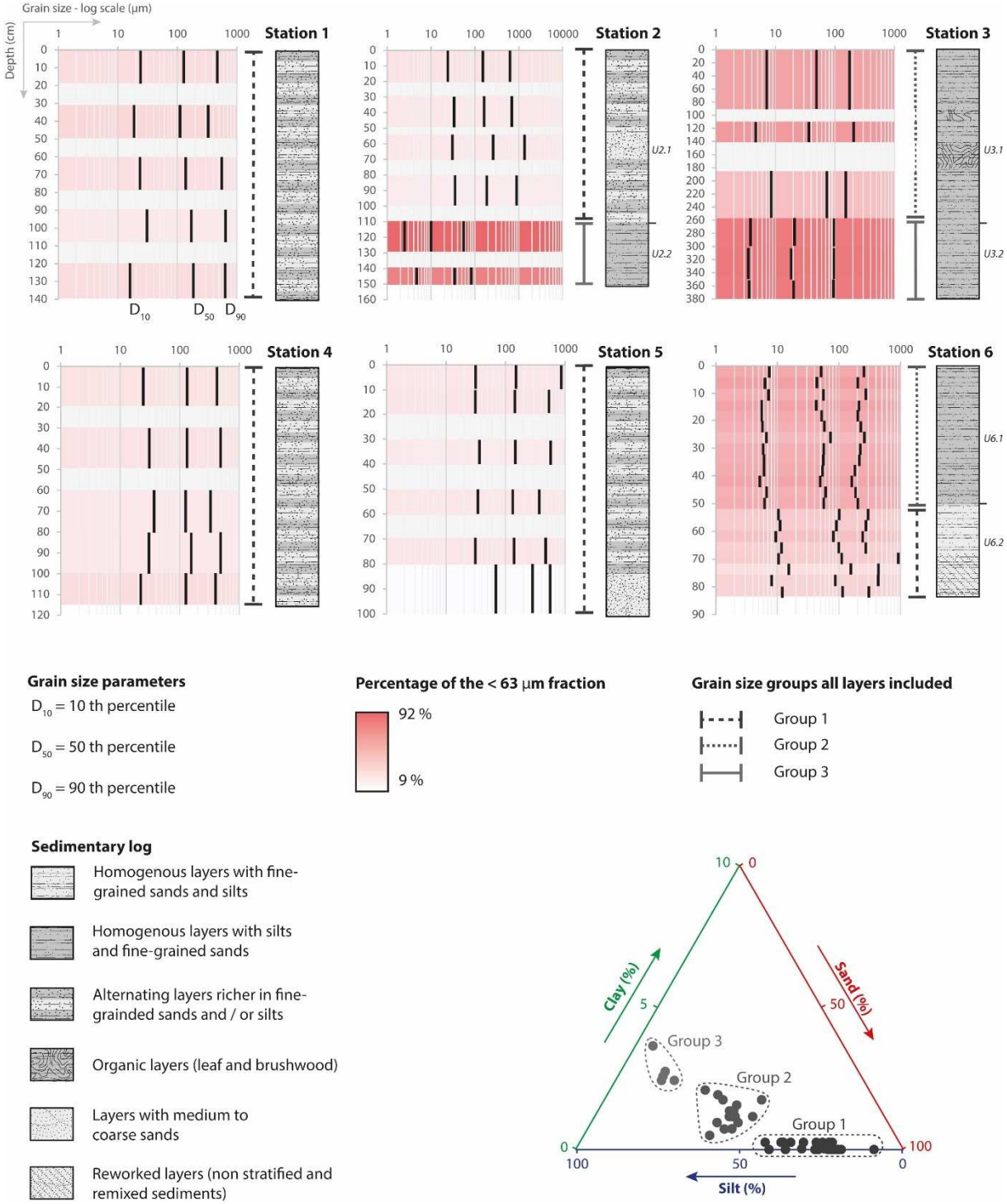

Figure 2. Sedimentological analysis of Bienne riverbank sediments. Sampling stations numbered from upstream to downstream along the river straight. Vertical bars show grain-size parameters over the analyzed layers.

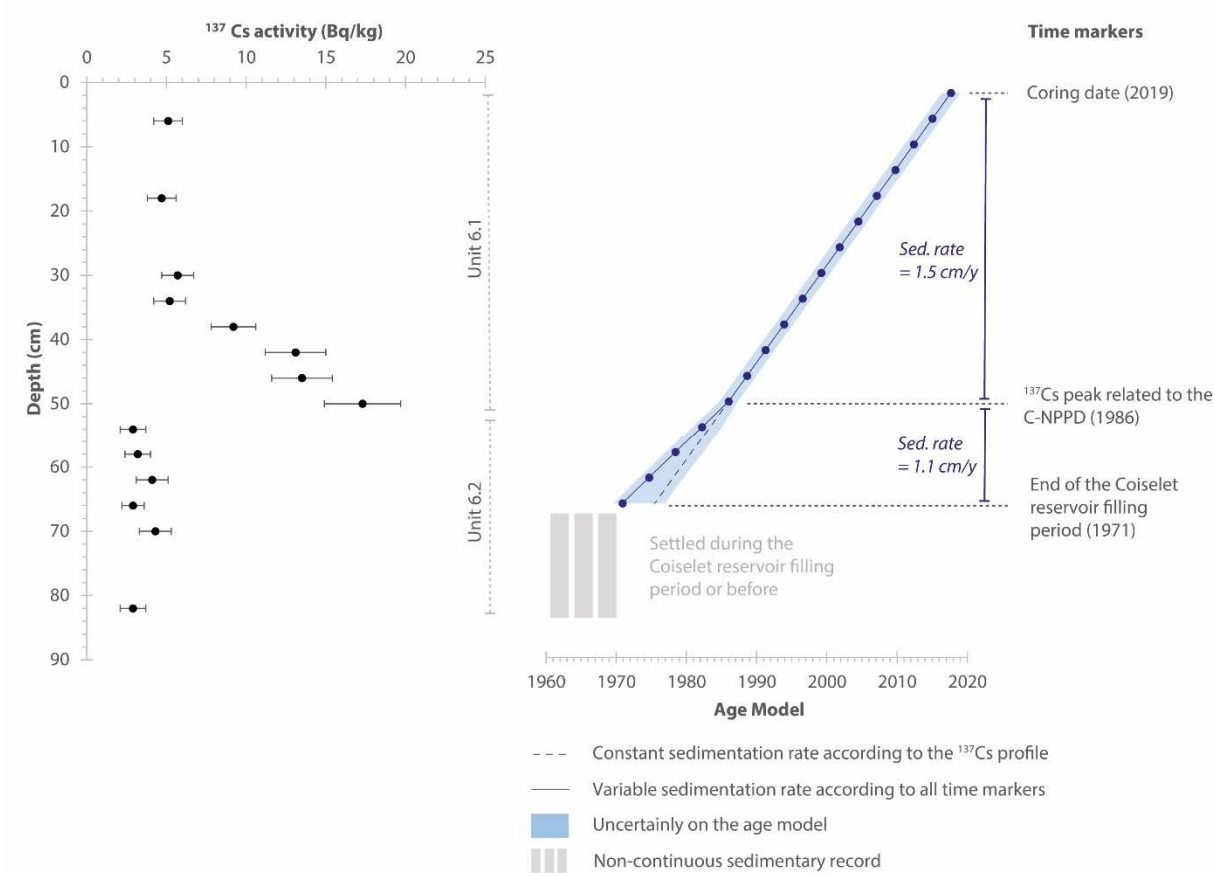

Figure 3. The ^{137}Cs profile and the age model defined in the sedimentary core sampled at station 6 (C-NPPD = Chernobyl Nuclear Power Plant Disaster). The sediment core is composed of 2 units (sedimentary groups 1 and 2, see Fig. 2). The sedimentary transition at 52 cm of depth can be explained by changes in the riverbank functioning, which occurred during the early 1980s and probably related to the water level management of the Coiselet Dam. The bottom part of unit 2 (68–84 cm) presents sedimentary evidence of a non-continuous record (flood deposits and/or sediment reworking). This sedimentary pattern was interpreted as deposited during or before the filling period of the reservoir. Possible erosional episodes may have occurred during the deposition of unit 2.

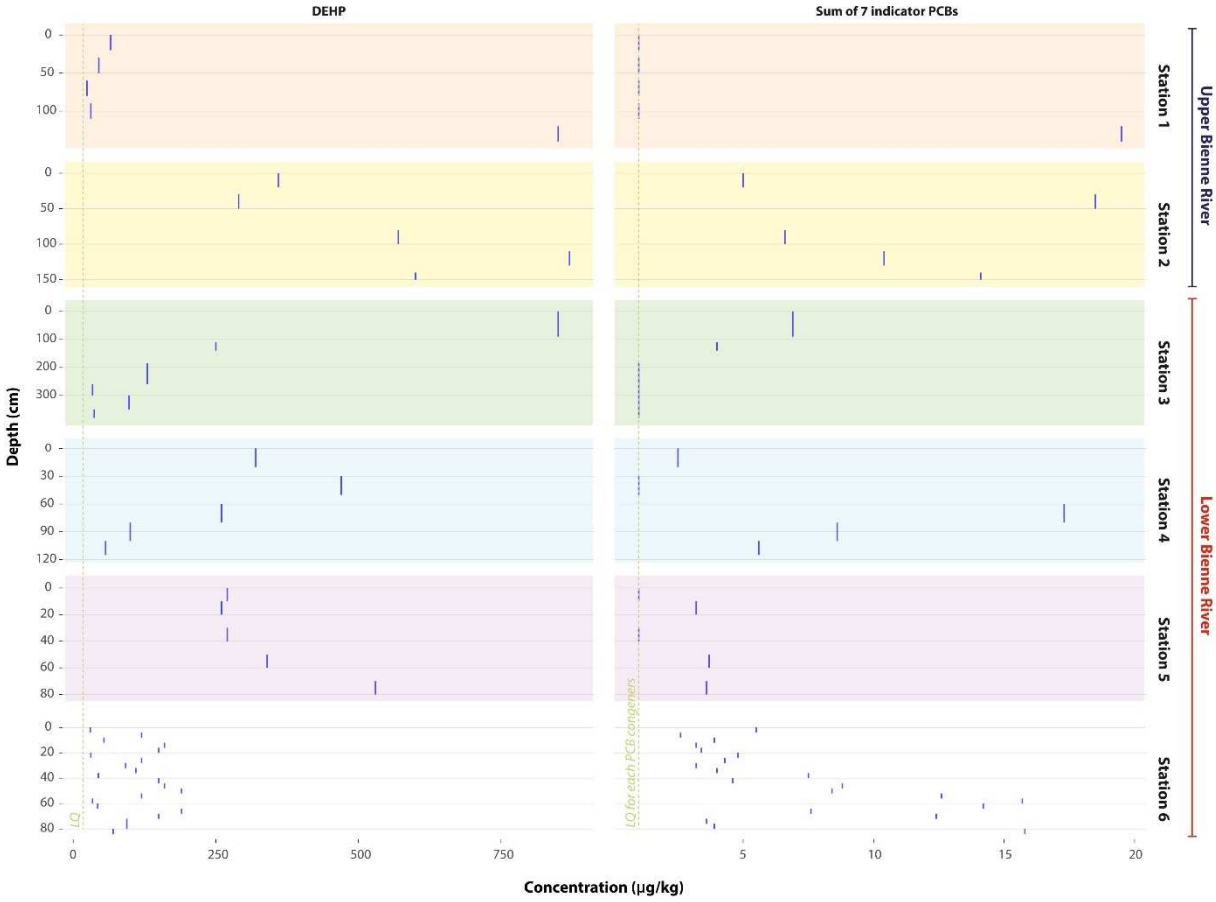

Figure 4. Sedimentary concentrations of DEHP and sum of 7 indicator PCBs in sediment layers collected in riverbank profiles (stations 1 to 5) and the core (station 6). In this study, they are considered as chemostratigraphic markers of the Anthropocene. LQ = limit of quantification. Concerning the sum of the 7 indicator PCBs, some sedimentary layers attest to concentrations under the LQ for all congeners, but PCBs are detected in concentrations ranging between 0.5 and 1 µg/kg.

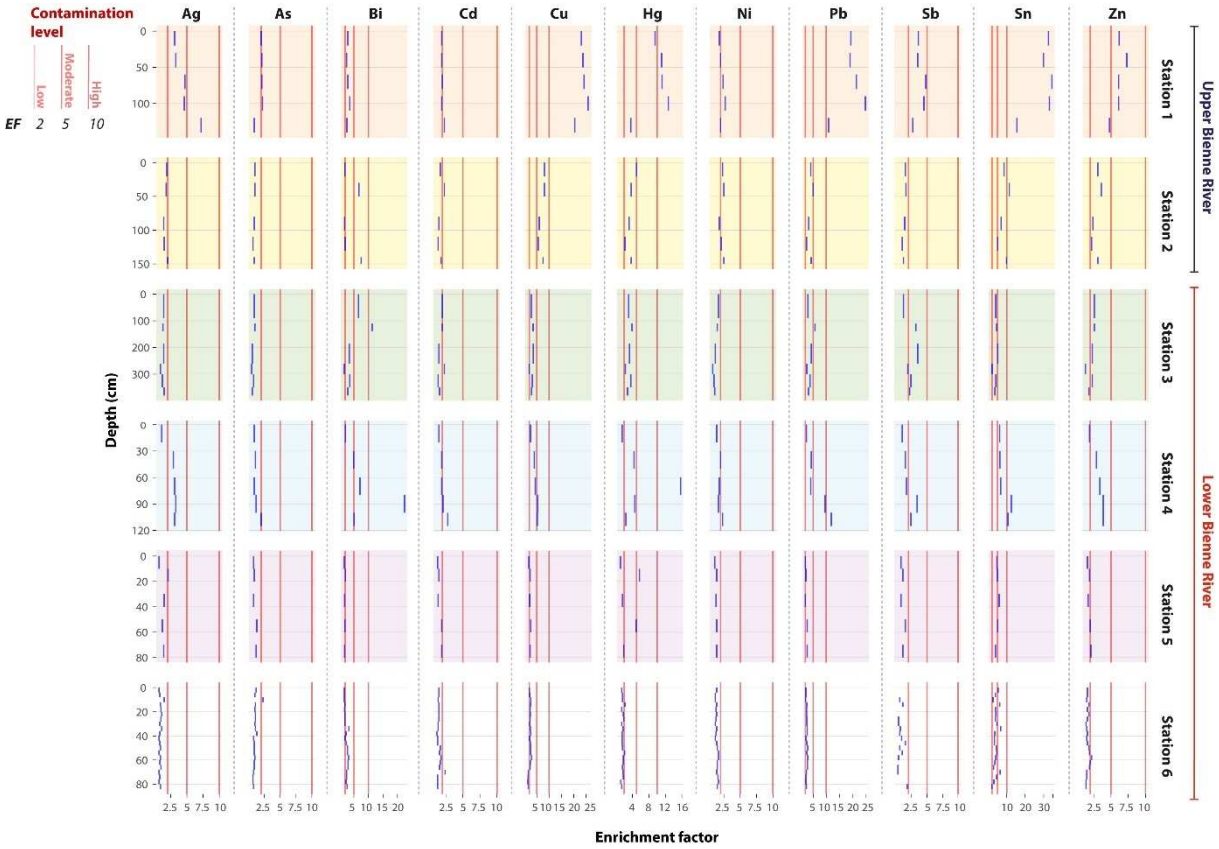

1141

1142 Figure 5. Trace element contaminant levels based on enrichment factors (EF, see text for calculation)
1143 in riverbank sediments at the six studied stations.

1144

1145

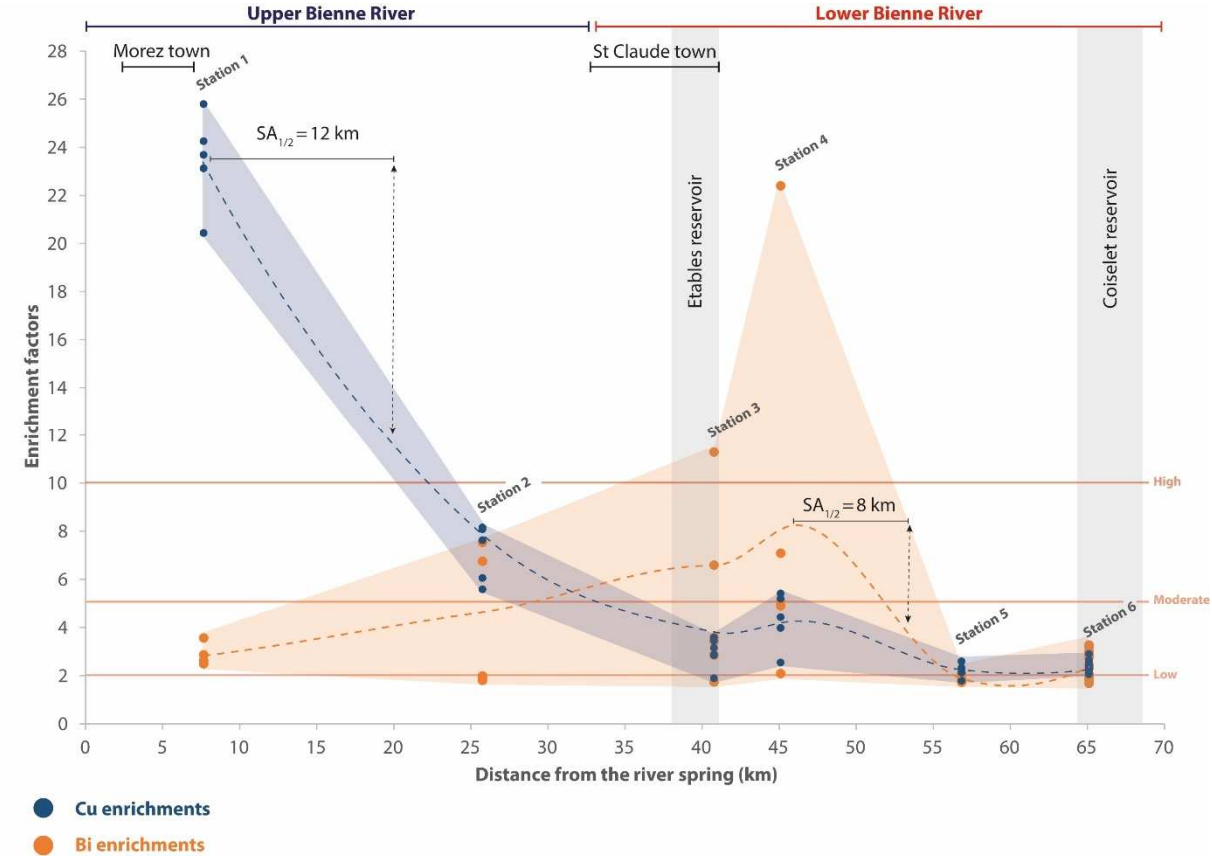

1146

1147 Figure 6. Spatial distribution of Cu and Bi enrichment factors (EF) in riverbank sediments. For each
1148 station, EF distributions are shown with colored dots. The Cu distribution is representative of a TE
1149 group composed of Ag, As, Cu, Hg, Pb, Sb, Sn, and Zn. Bi has spatial distribution different from other
1150 TEs. Blue and green envelops delimit minimum and maximum for Cu and Bi enrichments in all
1151 stations. Blue and green dolt lines represent loess smoothing curves (span = 0.75) for Cu and Bi
1152 enrichments. The spatial attenuation ($SA_{1/2}$) corresponds to the distance necessary to decrease
1153 enrichments by a factor 2 downstream peaks.

1154

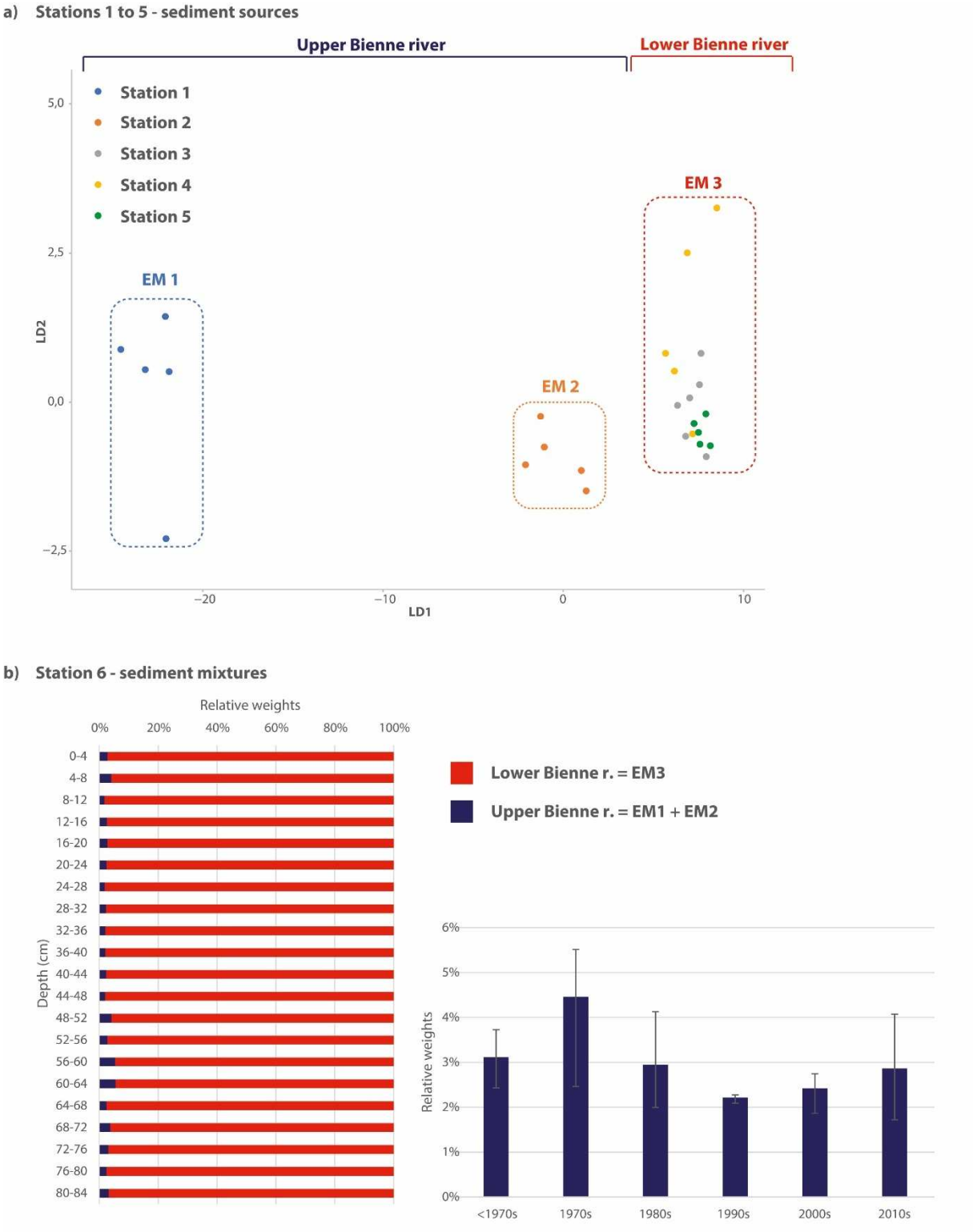

Figure 7. Result of the fingerprinting procedure FingerPro, performed with Trace element/Al ratios. Cu, Pb, and Zn were selected as the best tracers. a) The Linear Discriminant Analysis (LD) led to the characterization of three endmembers (EM) corresponding to station 1 for EM1; station 2 for EM 2; and stations 3, 4, and 5 for EM3. b) The mixing model evaluation of the relative weights of the three endmembers in the sedimentary mixtures at the river outlet (station 6). Results are shown for each sediment layer of the core and average values of the Upper Bienne River weights by decades according to the age model.

1163

Station	Ag	As	Bi	Cd	Cr	Cu	Hg	Mo	Ni	Pb	Sb	Sn	W	Zn	DEHP	PCBs
Station 1	1.0-2.8	8.8-19.0	0.4-0.6	0.5-0.7	11.7-15.1	300.0-359.0	0.19-0.56	0.7-1.0	17.6-27.6	212.0-412.0	1.4-2.0	28.0-50.5	71-87	254.0-310.0	24-850	<1-19.5
Station 2	0.6-0.9	8.8-9.9	0.3-1.6	0.5-0.7	14.7-19.7	107.0-135.0	0.15-0.23	0.8-1.0	23.5-34.4	64.4-92.1	0.7-0.8	12.3-19.3	88-108	145.0-187.0	290-870	5-18.5
Station 3	0.5-0.6	5.2-10.9	0.5-2.3	0.4-1.1	10.7-14.8	37.1-58.6	0.13-0.21	0.5-1.1	12.0-18.4	46.1-115.0	0.5-1.7	5.7-8.3	53-106	94.3-149.0	34-850	<1-6.9
Station 4	0.3-1.0	6.5-8.7	0.3-3.3	0.3-0.5	7.3-17.9	27.0-66.1	0.04-0.66	0.4-0.8	8.9-17.7	35.6-137.0	0.4-1.3	6.1-16.8	41-82	67.4-159.0	57-470	<1-17.3
Station 5	0.2-0.6	6.1-6.5	0.2-0.3	0.3-0.3	9.1-11.7	19.6-26.7	0.04-0.21	0.5-0.6	8.8-12.2	26.6-30.1	0.3-0.4	3.6-7.7	39.5-1	56.6-74.6	260-530	<1-3.7
Station 6	0.1-0.4	4.5-14.2	0.2-0.4	0.1-0.4	8.3-17.2	20.4-25.8	0.04-0.06	0.3-07	7.7-13.2	22.9-33.6	0.1-0.5	1.8-6.6	<10-83	42.4-65.7	30-190	2.6-15.7

1164 Tab. 1. Ranges of trace element concentrations in sediments collected in stations 1 to 6 (in mg/kg)

Basin	Ag	As	Bi	Cd	Cr	Cu	Hg	Mo	Ni	Pb	Sb	Sn	W	Zn
Bienne[1]	0.3	7.8	0,2	0.2	11.5	12.6	0.04	0.5	9.4	14.9	0.4	1.4	77	42.3
Rhône[2]				0.06-0.24	14-56	0-26			0-68	4-22				4-95
Loire[3,4]	0.2	19.4-46.8	0.6-1.1	0.3-1.1	88-110	14-27	0.02-0.09	0.3-1.1	28.4	33-69	0.3-2.4	7-17	5.1-7.4	90-139
Seine[5]				0.2	40	14	0.02			20				60
Garonne[6]				0.5	23	25			12	18				78

1165 Tab. 2. Trace element concentrations in sediment collected at the base of the old floodplain
1166 downstream of the station 6 and comparison with pre-industrial concentration ranges in
1167 neighborhood basins (in mg/kg), 1 = this study, 2 = Dendeviel et al, 2020b (Upper Rhône, with an
1168 *aqua regia* digestion), 3 = Dhivert et al, 2015b, 4 = Grosbois et al 2020, 5 = Meybeck et al, 2004, 6 =
1169 Grousset et al, 1999.

	Depth (cm)	Ag	As	Bi	Cd	Cr	Cu	Hg	Mo	Ni	Pb	Sb	Sn	W	Zn	
Station 1	0-20	3.1	2.0	2.9	1.9	1.0	23.1	9.5	1.3	1.8	19.4	3.6	32.6	1.0	6.2	
	30-50	3.3	2.1	2.5	1.9	1.0	23.7	11.1	1.4	2.0	19.1	3.5	29.9	1.0	7.3	
	60-80	4.7	2.1	2.9	2.0	1.0	24.2	11.2	1.6	2.4	21.5	4.8	34.5	1.0	6.1	
	90-110	4.6	2.2	3.6	1.9	1.0	25.8	12.7	1.4	2.7	25.0	4.5	33.1	1.0	6.1	
	120-140	7.2	0.9	2.6	2.3	1.0	20.4	3.6	1.4	2.0	10.9	2.7	15.5	0.7	4.8	
Station 2	0-20	1.9	1.0	1.9	1.7	1.1	8.1	5.0	1.3	2.3	4.1	1.5	8.5	1.0	3.1	
	30-50	1.8	1.0	6.7	2.3	1.2	8.1	3.7	1.3	2.5	5.0	1.6	11.3	1.1	3.6	
	80-100	1.4	0.9	1.8	1.5	1.0	6.0	3.2	1.3	1.8	3.3	1.4	7.0	1.0	2.4	
	110-130	1.5	0.7	2.0	1.4	0.9	5.6	2.2	1.1	2.1	2.5	1.0	5.1	0.7	2.2	
	140-150	2.0	0.9	7.5	1.8	1.2	7.6	3.7	1.1	2.5	4.2	1.2	9.9	0.9	3.1	
Station 3	0-90	1.4	0.9	6.6	2.0	1.1	2.8	3.1	1.0	1.7	3.0	1.2	4.0	0.7	2.6	
	110-140	1.3	1.0	11.3	2.0	1.0	3.5	3.9	1.6	1.5	5.7	3.2	4.5	1.0	2.6	
	185-260	1.4	0.6	3.4	1.5	0.8	3.6	3.3	0.7	1.2	4.3	3.5	5.2	0.6	2.3	
	260-300	0.9	0.5	1.7	2.3	0.7	1.9	2.3	0.5	0.8	2.6	1.9	2.1	0.7	1.3	
	300-350	1.2	0.8	3.6	1.4	0.8	3.2	3.6	0.7	1.0	3.8	2.4	4.1	1.0	2.3	
	350-380	1.5	0.6	2.9	1.6	0.8	2.9	2.8	0.8	1.1	3.2	2.2	3.6	0.6	1.8	
Station 4	0-20	1.1	0.9	2.1	1.5	1.2	2.5	1.5	1.2	1.4	2.4	1.0	6.1	0.7	1.9	
	30-50	2.9	1.1	4.9	1.9	1.4	4.0	4.4	1.7	2.0	4.3	1.5	6.3	0.9	2.9	
	60-80	3.1	0.9	7.1	1.9	1.4	4.4	15.7	1.0	1.8	4.1	1.7	6.7	0.6	3.4	
	80-100	3.3	1.2	22.4	2.1	1.6	5.4	4.6	0.9	1.7	9.5	3.4	12.5	1.1	3.9	
	100-115	3.1	2.0	5.1	2.8	1.5	5.2	2.4	1.8	2.3	11.9	2.4	10.7	1.3	3.9	
Station 5	0-10	0.7	0.8	1.7	1.3	1.0	1.8	1.1	1.2	1.1	2.0	0.8	4.7	0.6	1.6	
	10-20	2.1	0.9	2.1	1.5	1.1	2.3	5.7	1.2	1.4	2.2	1.1	5.0	0.6	1.9	
	30-40	1.5	0.8	1.8	1.4	1.1	2.1	1.6	1.2	1.3	2.0	0.8	5.9	0.5	1.7	
	50-60	1.2	1.3	1.9	1.9	1.2	2.6	4.9	1.4	1.4	2.7	1.5	5.1	1.0	2.0	
	70-80	1.4	1.2	1.8	1.9	1.2	2.3	1.9	1.4	1.4	2.7	1.1	3.9	1.0	2.1	
Station 6	0-4	0.7	1.2	1.7	1.5	1.2	2.0	1.4	1.2	1.4	2.2		5.3		1.6	
	4-8	0.8	1.0	1.7	1.5	1.1	2.1	1.6	1.2	1.2	2.2		3.8	1.3	1.6	2010s
	8-12	1.5	2.3	1.7	1.4	1.9	2.6	1.6	1.1	1.2	2.1	0.6	2.5	1.2	1.5	
	12-16	0.9	1.1	1.9	1.5	1.1	2.5	2.2	1.2	1.4	2.6	1.1	6.2	0.5	1.8	
	16-20	1.0	1.0	1.8	1.5	1.1	2.3	1.4	1.2	1.3	2.5		3.9	1.3	1.6	2000s
	20-24	1.1	1.1	1.9	1.5	1.1	2.4	1.8	1.2	1.4	2.5		4.1	1.2	1.8	
	24-28	1.0	1.1	1.9	1.5	1.2	2.3	1.9	1.4	1.3	2.6	0.4	3.8	1.3	1.6	
	28-32	0.8	1.0	1.9	1.4	1.0	2.2	1.4	1.1	1.2	2.6	0.4	4.7	1.3	1.4	
	32-36	1.1	1.1	3.3	1.4	1.1	2.4	1.7	1.2	1.4	2.7	0.7	6.7	1.3	1.5	1990s
	36-40	0.8	1.3	2.3	1.2	1.2	2.6	1.5	0.9	1.3	2.7	0.6	3.5	1.3	1.6	
	40-44	0.7	0.8	2.0	1.3	0.9	2.1	1.5	1.4	1.2	2.3	0.9	3.3	0.9	1.5	
	44-48	0.8	0.9	2.4	1.3	1.0	2.4	1.5	0.9	1.4	2.6	1.5	3.3	0.7	1.6	
	48-52	0.9	0.9	2.8	1.7	1.1	2.5	1.6	1.1	1.5	2.9	0.6	4.3	1.3	1.8	1980s
	52-56	0.7	0.9	2.8	1.6	1.1	2.5	2.1	1.0	1.7	2.6	1.0	4.6	0.8	1.9	
	56-60	0.9	1.0	3.2	1.8	1.3	2.9	1.8	1.1	1.7	2.9	0.4	4.0	1.5	2.2	
	60-64	0.8	0.9	3.0	1.7	1.2	2.4	1.8	1.0	1.5	2.8		3.6	1.2	2.0	1970s
	64-68	1.0	0.9	3.0	1.6	1.2	2.3	1.6	0.9	1.5	2.8	0.3	2.9	1.3	1.9	
	68-72	0.7	0.8	2.5	2.4	1.1	1.6	1.7	0.9	1.4	2.4	0.3	6.4	1.3	1.5	
	72-76	0.8	0.7	2.5	1.3	1.2	1.5	1.8	0.9	1.6	2.3		4.5	1.3	1.5	<1970s
	76-80	0.7	0.7	2.3	1.3	1.1	1.4	1.2	1.0	1.7	2.2		3.0	1.3	1.4	
	80-84	0.9	0.8	2.7	1.3	1.1	1.6	1.4	0.9	1.5	2.4	1.8	1.9	0.6	1.4	

Tab. 3. Trace element enrichment factors (EF) in riverbank sediments at the six studied stations (see text for calculation). The color gradient represents contamination levels: negligible (EF < 2), low (EF between 2 and 5), moderate (EF between 5 and 10 and high (EF > 10).